TAMPEREEN TEKNILLINEN YLIOPISTO
TAMPERE UNIVERSITY OF TECHNOLOGY

NIKTA POURNOORI

WIRELESS MONITORING OF A CHARGE STORAGE IN AN RF ENERGY HARVESTING DEVICE

Master of Science Thesis

Examiner: Academy Research Fellow Toni Björninen and Doctoral Student Muhammad Waqas Ahmad Khan
Examiner and topic approved by the Council of the Faculty of Computing and Electrical Engineering on 3 January 2018

ABSTRACT

NIKTA POURNOORI: Wireless Monitoring of a Charge Storage in an RF Energy Harvesting Device
Tampere University of Technology
Master of Science Thesis, 67 pages
January 2018
Master's Degree Programme in Computing and Electrical Engineering
Major: Electronics
Examiner: Academy Research Fellow Toni Björninen and Doctoral Student Muhammad Waqas Ahmad Khan

Keywords: RF energy harvesting, RF rectifier, RF switch, Passive UHF RFID tag, Impedance matching network, Dipole antenna

Today's advancements in modern technologies have grown the demand of low power wireless application devices usage. Using the batteries in any portable electronic devices results in a limitation in occupying the space and declining the lifetime of the application devices. Hence, one of the significant challenges in low power wireless technologies is providing the energy sources that are able to supply the required power for operating wireless devices continuously without degrading their performance. Energy harvesting is a growing interest technique to harvest ambient energy from renewable sources such as vibration, solar light, wind, thermal, and electromagnetic wave (EM) and convert these energies into useable electrical energy. Harvesting ambient energy from electromagnetic wave known as the RF energy harvesting is becoming increasingly important for powering the battery-less electronics devices and passive RFID tags. Indeed, this kind of power is readily available especially in HF and UHF frequencies due to the presence of propagating radio waves of wireless technologies such as cellular, TV, radio, satellites, and Wi-Fi signals in environment. Thus, it can be considered as a promising solution to meet the required of the battery replacement and providing a power supply over very long periods.

In this project, a radio frequency (RF) energy harvesting unit integrating a passive UHF RFID tag as a charge storage indicator is presented. In this system, an energy harvesting unit converts the RF signal to DC and charges a storage capacitor. In addition, to transfer the maximum power through the system, an impedance matching network is designed between the RF power source and the RF rectifier. The RF switch, consists of a pin diode and UHF RFID tag, monitors the capacitor voltage. When the voltage across the capacitor terminals approaches 0.633 V, signal is transmitted to the RFID reader. The proposed RF energy harvesting system operates at European UHF RFID spectrum from 865.7 MHz to 867.7 MHz, which the frequency of 866 MHz is considered as our target frequency in this study. All the procedure of designing, simulation and fabrication are explained in details and the experimental results indicate that 0.633 V at the terminals of the storage capacitor can be achieved with −5.5 dBm of the RF input power applied into the energy harvesting unit.

PREFACE

All of the work presented in the master thesis “Wireless Monitoring of a Charge Storage in an RF Energy Harvesting Device”, is conducted at the research group of Wireless Identification and Sensing System (WISE) in Tampere University of Technology from May 2017 to January 2018. The research work of this project has been supported by Academy of Finland and TUT foundation.

I would like to thank my thesis examiner and supervisor, Dr. Toni Björninen for all of his supports, guidance, and insightful ideas and comments. I really appreciate him providing me with the opportunity to work in his research group and complete my thesis. I also wish to thank my examiner Muhammad Waqas Ahmad Khan for his generous help, keen insight and for everything he has taught me during this research. I am also thankful to all my colleagues in the WISE Group for their help and support.

Moreover, I would like to express my sincerest appreciation to my lovely husband, Keivan, for his patience, endless kindness and continuous support through all the time of my studies.

Finally, I would like to thank my great parents and my sisters, Negin and Nazanin, for all their unconditional love, prayers, teaching and motivations through my life.

Tampere, January 2018

Nikta Pournoori

CONTENTS

LIST OF FIGURES

LIST OF TABLES

LIST OF SYMBOLS AND ABBREVIATIONS

A	Ampere
ADS	Advance Design System
AR	Axial Ratio
cm	Centimeter
CMOS	Complementary Metal Oxide Semiconductor
CW	Continuous Wave
dB	Decibel
DC	Direct Current
EDLC	Electrochemical Double-Layer Capacitor
EH	Energy Harvesting
EIRP	Effective Isotropic Radiated Power
EM	Electromagnetic
E- Plane	A two-dimensional representation of the radiation pattern which contains only electric field and maximum radiation direction.
ESR	Equivalent Series Resistance
FET	Field Effect Transistor
FNBW	First Null Beam Width
GHz	Giga Hertz
GND	Ground Plane
HB	Harmonic Balance
HF	High Frequency
HFSS	High Frequency Structure Simulator
HPBW	Half Power Beam Width
H-Plane	A two-dimensional representation of the radiation pattern which contains only magnetic field and maximum radiation direction.
Hz	Hertz
I	Intrinsic layer
IC	Integrated Circuit
IEEE	Institute of Electrical and Electronics Engineers
IoT	Internet of Things
LAN	Local Area Network
LF	Low Frequency
LIB	Lithium-Ion Battery
LIP	Lithium- Ion Polymer
LSSP	Large-Signal S-Parameter
MEMS	Micro Electro Mechanical System
MHz	Mega Hertz
MOSFET	Metal Oxide Semiconductor Field-Effect Transistor
mm	Millimeter
PCB	Printed Circuit Board
PCE	Power Conversion Efficiency
PIE	Pulse-Interval Encoding
PLF	Polarization Loss Factor
RCS	Radar Cross Section
RF	Radio Frequency
RFID	Radio Frequency Identification
RRE	Radar Range Equation
SHF	Super High Frequency

S-parameters	Scattering parameters
SPDT	Single-Pole Double-Throw
SPST	Single-Pole Single-Throw
SWR	Standing Wave Ratio
TUT	Tampere University of Technology
UHF	Ultra High Frequency
VNA	Vector Network Analyzer
Wb	Weber
WPT	Wireless Power Transfer
WSN	Wireless Sensor Network
3D	Three Dimensional
µm	Micrometer
Ω	Ohm
B	Magnetic flux density [Wb/ m^2]
C	Capacitor per until length [F/m]
c	Velocity of light [m/s]
D	Electric displacement [C/ m^2]
D	Directivity of antenna [dBi]
E	Electric field [V/m]
F	Electric force [N]
f	frequency [Hz]
G	Conductance per unit length [S/m]
G	Gain of antenna [dBi]
H	Magnetic field [A/m]
I	Current [A]
I(z)	Current wave in z direction [A]
J	Current density [A/ m^2]
k	Radiation efficiency of antenna
L	Inductance per unit length [H/m]
P	Vector polarization [C/ m^2]
P	Power [J/s]
Q	Electric charge [C]
R	Resistance per unit length [Ω/m]
R_A	Resistance of antenna [Ω]
RL	Return loss [dB]
T	Temperature [Kelvin]
V(z)	Voltage wave in z direction [V]
W	Width [mm]
W_e	Electric energy [J]
W_m	Magnetic energy [J]
W_i	Incident power density [W/m^2]
W_s	Scattered power density [W/m^2]
X_A	Reactance of antenna [Ω]
Z_0	Characteristic Impedance [Ω]
Z_A	Impedance of antenna [Ω]
α	Attenuation Constant [Np/m]
β	Propagation Constant [Np/m]
γ	Complex propagation Constant [Np/m]
Γ	Reflection coefficient
Γ*	Conjugate-matched reflection coefficient

e_r	Reflective efficiency
e_{rad}	Radiation efficiency
e_o	Total efficiency
δ	Skin depth [m]
δ_e	Electric loss angle
δ_m	Magnetic loss angle
ε	Permittivity of medium [F/m]
ε'	Real part of permittivity
ε''	Imaginary part of permittivity
ε_r	Relative permittivity of medium
ε_0	Permittivity of free space [F/m]
ε_{eff}	Effective Relative Permittivity
$\eta_{matching}$	Matching efficiency
θ	Azimuthal angle in spherical coordinate system
λ	Wave length [m]
μ	Permeability of medium [H/m]
μ'	Real part of permeability
μ''	Imaginary part of permeability
μ_r	Relative Permeability
μ_0	Permeability of free space [H/m]
ρ	Electric charge density [C/m^3]
σ	Conductivity [S/m]
σ_e	Effective conductivity
φ	Polar angle in spherical coordinate system
τ	Power transfer coefficient
ω	Angular Frequency [rad/s]
Ψ_p	Angle difference

1. INTRODUCTION

Nowadays, one of the most significant issues is energizing the low power wireless application devices. Since enhancing the lifetime of required battery to maintain the operation of these devices is still impractical, harvesting the energy from ambient sources have become a promising solution to power the portable electronic devices [Publication I]. One of the most popular technique to extract the power from ambient energy is the RF energy scavenging from the electromagnetic wave (EM). Due to readily available of this type of energy harvesting, a sustainable power supply can be provided for any wireless devices. Thus, this method can be found quickly in several types of research in any forms of wireless applications such as Wireless Body Networks (WBN), Wireless Sensor Networks, and wireless charging systems. The method of Wireless Power Transfer (WPT) can be divided into three different categories including the RF energy transfer and harvesting, resonant inductive coupling, and magnetic resonance coupling. The two techniques of resonant inductive coupling, and magnetic resonance coupling, which contain the high power density and conversion efficiency, are suitable for near field. Thus, the effective distance for these both method can vary from a few millimeters to a few meters. As these techniques need to calibrate and align the coils/resonator at receivers and transmitters, they are not appropriate for the mobile or recharging systems. In contrast, the RF energy harvesting can solve such limitation. The transmitting RF energy is considered for the far field power transfer. Although, RF power transfer includes lower efficiency of converting the RF signal to DC compared to other methods, it can be used for a large number of devices, which are located in a wide area. The strength of the signal for transmitting the RF power in a far field is dependent on the distance between the transmitter and receiver [1].

In general, an RF energy harvesting system consists of an RF power source, impedance matching network, a single/multi stage RF rectifier as a key component and an energy storage unit. To perform RF to DC conversion at UHF bands, several researches have been done on the structure of the RF energy harvesting system particularly the rectifier architectures. The different topologies have been studied for designing the RF rectifier including Villard/Dickson charge pump [2][3], Schottky diode with low threshold voltage [4] and CMOS compatible MOSFET with zero threshold voltage. Hence, the passive devices can capture sufficient DC power delivered from the incoming RF power and operate at the desired frequency [2][3][Publication I]. In this work, by using the Dickson topology two-stage charge pump based on the Schottky diodes is configured as the RF rectifier and in order to maximize the power transmission through the energy harvesting system, an L-matching impedance network including two RF inductors is offered. To configure the RF

switch, which comprises of a pin diode and RFID tag, a series SPST switch structure of PIN diode is employed. Moreover, this research is simulated and tested at the operating frequency of 866 MHz as the frequency range of the European UHF RFID. To achieve the experimental results, this circuit is implemented on the FR4 substrate. Therefore, the performance of the whole designed system is evaluated by measuring the output DC voltage of the RF rectifier and turning ON the RF switch to get a response of the RFID IC.

This Master of Science Thesis is organized in the following manner. Chapter 2 defines the essential theory of the RF energy harvesting system. Chapter 3 explains the theory of the RF switch and introduces the PIN diode principles and its structures as a switch. Chapter 4 describes the basic theoretical background including the electromagnetic wave theory, antenna theory, and the RFID system fundamentals. Chapter 5 presents the scope of this thesis and the main topic, which is provided by the design procedures, simulation, and measurement results. Finally, all these efforts are concluded in chapter 6.

2. BASIC THEORY OF RADIO – FREQUENCY ENERGY HARVESTING SYSTEMS

2.1 Overview of the RF Energy Harvesting

Energy harvesting is a technique of converting ambient energy into usable electrical energy to drive electronics devices. In a similar viewpoint, energy harvesting systems capture the natural (renewable) energy, accumulate this energy and store it for later use [5]. There are various types of renewable energy sources to harvest energy such as vibration, solar light, wind, thermal, and electromagnetic wave (EM). Harvesting ambient energy, also known as an energy scavenging, from the electromagnetic wave (EM) is referred to as RF energy harvesting [6]. Among the multiple ambient energy resources, RF energy harvesting has recently attracted the most significant attention. This type of energy is readily available especially in HF and UHF frequencies due to the deployment of wireless technologies such as cellular, TV, radio, satellites, and Wi-Fi signals [7]. Furthermore, it is a promising solution for providing a power supply over very long periods [8]. Hence, it can overcome the need for battery replacement, which is inconvenient economically and practically [9]. Since, the renewable energy has developed gradually to contain the micro power harvesting, the ambient RF energy harvesting can be realized to partially/fully supply the power required for low power devices such as wearable electronics devices, RFID systems, medical implantable devices, wireless sensor network (WSN), and internet of things (IoT) [3] [10] [Publication I].

The concept of wireless power harvesting and transmit dates back to the work of Tesla and Heinrich Hertz over 100 years ago [9]. According to this concept, the wireless energy converts to the direct current (DC) power, when the wireless power radiates into free space. The wireless power transfer (WPT) contains two major types: near-field and far-field systems. To transfer wireless power in near-field systems, a magnetic resonance or electric/magnetic induction is employed. This kind of power transmission has high efficiency but it is appropriate for short ranges of energy harvesting systems. For transmitting power wirelessly in far-field, the energy harvesting devices consist of antennas to capture the propagated electromagnetic waves and rectifiers/charge pumps based on diode/transistor technology used for converting RF powers to DC power [7].

In addition, some challenges that researchers face, is the development of an efficient, achieving sufficient output voltage and the sensitivity of the RF energy harvesting systems. It needs to make a tradeoff among these parameters to achieve an effective system for a certain purpose.

Figure 1 demonstrates the main functional blocks of an RF energy harvesting system. It comprises of an RF power source, a matching network, a single/multi stage rectifier and a charging control unit. A rectifier and charging control unit can harvest RF signals from free space, convert it to DC voltage, and store the achieved DC voltage by charging a capacitor. The details of each block are explained subsequently.

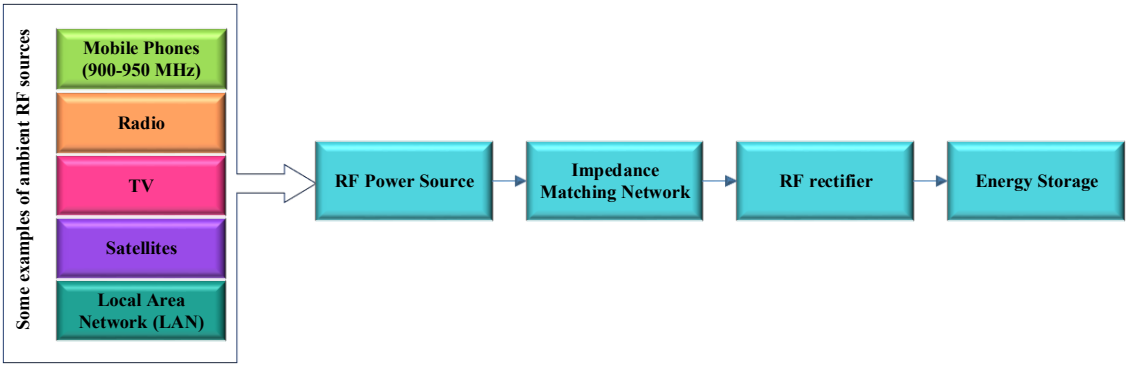

Figure 1. *General block diagram of an RF energy harvesting system*

2.2 RF Power Source

In general, the RF power source is an antenna that picks up electromagnetic waves. The various sources, from which an RF antenna can capture the power; contain UHF signals, mobile phones (900-950MHz), or Local Area Network (LAN) for 2.45GHz/5.8 GHz [11]. The equivalent device of an antenna is an RF signal generator, which can be used in the prototype measurements, to maintain a stable continuous wave (CW) and accurate input signal for conversion, as we used in our study.

2.3 Impedance Matching Network and Transmission Lines

Impedance matching network is an essential part to optimize the performance of the whole system and maximize the power transmission. Impedance mismatch power loss occurs when the impedance of the load (energy harvesting system) is not equal to the complex conjugate impedance of the RF source (antenna). In this context, the RF rectifier cannot absorb all the RF incident power, hence, a part of incident power will be reflected back. Thus, the available power for rectification is decreased and the power conversion efficiency (PCE) will be degraded [1] [2] [12].

Since the rectifier is inherently a nonlinear device, the input impedance of the rectifier will vary as a function of both frequency and incident power. Therefore, it is difficult part of designing in an RF energy harvesting system [12]. The most common architecture utilized for matching network includes an L, a Π and a T networks, which contain reactive components [13]. To design the matching network, the matching efficiency ($\eta_{matching}$)

term is introduced. It expresses how the antenna is matched well to the RF rectifier of the energy harvesting system. The matching efficiency is given by [14],

$$\eta_{matching} = 1 - |\Gamma|^2 \tag{2.1}$$

where Γ denotes the reflection coefficient of the power wave, which can be calculated by,

$$\Gamma = \frac{Z_{rectifier} - Z^*_{antenna}}{Z_{rectifier} + Z_{antenna}} \tag{2.2}$$

As discussed earlier, with an impedance $Z_{rectifier} = Z^*_{antenna}$, where (*) indicates the complex conjugate; the matching efficiency will obtain the maximum value [14].

Transmission line theory is related to the electrical size that means when the physical dimension of a network can be compared with the signal wavelength. In this state, analyzing the circuit utilizing the circuit theory is infeasible; thereby, it needs to distribute the elements of the circuit along the line. The lumped-element equivalent circuit of a short transmission line, as shown in Figure 2, presents a solution of the circuit parameters [15].

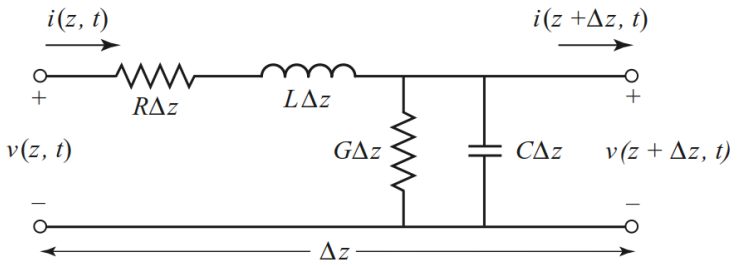

Figure 2. *Lumped-element equivalent circuit of short transmission line [15]*

Two wave equation can be used to obtain the voltage and current of the circuit as expressed in following equations [15],

$$V(z) = V_0^+ e^{-\gamma z} + V_0^- e^{\gamma z} \tag{2.3}$$

$$I(z) = I_0^+ e^{-\gamma z} + I_0^- e^{\gamma z} \tag{2.4}$$

where γ is the complex propagation constant, which can be calculated by [15],

$$\gamma = \alpha + j\beta = \sqrt{(R + j\omega L)(G + j\omega C)} \tag{2.5}$$

where R, L, G, and C are the quantities of per unit length defined as follow,

- R=Series Resistance per unit Length, for both conductors, in Ω/m.
- L=Series Inductance per unit Length, for both conductors, in H/m.
- G=Shunt Conductance per unit Length, in S/m.
- C= Shunt Capacitance per unit Length, in F/m.

The impedance of the line (Z_0) can be calculated by [15],

$$Z_0 = \frac{V_0^+}{I_0^+} = \frac{V_0^-}{I_0^-} = \sqrt{\frac{(R + j\omega L)}{(G + j\omega C)}} \tag{2.6}$$

By terminating the transmission lines with an arbitrary load, wave reflection will occurs in the location of the load due to mismatching of the transmission line and load impedance. The ratio of the incident voltage to its current at the load refers to Z_L. Therefore, the reflection coefficient in terms of the reflected voltages is expressed as [15],

$$\Gamma = \frac{V_0^-}{V_0^+} = \frac{Z_L - Z_0}{Z_L + Z_0} \tag{2.7}$$

The superposition of the incident and reflected waves can create a standing wave along the transmission line when $Z_L \neq Z_0$. Thus, the other parameter that can be measured the mismatch of the line and, hence, the reflection is standing wave ratio (SWR) described by [15],

$$SWR = \frac{V_{max}}{V_{min}} = \frac{1 + |\Gamma|}{1 - |\Gamma|} \tag{2.8}$$

Return Loss

In the state that the input impedance of the antenna is not matched properly to the impedance of the source, the transmitted power will be reflected back. Hence, Impedance matching of antennas is also measured with the input reflection coefficient or return loss (RL), which is referred to the reflected power. Return loss has the threshold equal to -10 dB, which is able to transmit 90% of the incident power. Return loss can be computed by [16],

$$RL\ (dB) = -20\, log|\Gamma| \tag{2.9}$$

where Γ denotes the reflection coefficient at the antenna input terminals, which is calculated by (2.2).

2.4 RF Rectifier

Rectifier is a key circuit block in an RF energy harvesting systems, which can convert the incoming RF signal from the antenna to the stable DC voltage and, hence, supply a circuit by using the power available at the RF antenna (source) terminals. Choosing the rectification circuit architecture depends on the received RF power level, the input frequency and the level of desired output DC voltage.The requirement characteristics of the rectifier to evaluate its performance contain the PCE, sensitivity, threshold voltage, circuit size, rise time, and ripple or noise, which are described subsequently [17].

The PCE of the rectifier is the ratio of the output DC power to the input power as shown in (2.10) [12].

$$\eta_{EH} = \frac{P_{outDC}}{P_{inEH}} \tag{2.10}$$

where P_{inEH} is the RF incident power and P_{outDC} denotes the output DC power across the load (Z_L) of the rectifier. The P_{outDC} can be represented as [12],

$$P_{outDC} = \frac{V_{outDC}^2}{Z_L} \tag{2.11}$$

In addition, the load of the rectifier can include a resistor, capacitor, inductor or a combination of all these components.

As discussed earlier, if the RF source is not matched properly to the rectifier, some energy will be reflected. However, this reflected power can be neglected only if the matching between the antenna and the rectifier is reasonably good. The input power can be calculated by [12],

$$P_{inEH} = P_{intot} - P_{reflected} \tag{2.12}$$

The minimum input power, which is necessary to attain the desired output DC power levels and ultimately reaching the highest efficiency, is called the sensitivity of the rectifier. To enhance the sensitivity performance and output voltage, it is required to utilize the rectifying elements with lower threshold voltage. Consequently, the threshold voltage of the rectifying components has the considerable effect on the efficiency [12].

Rise time is introduced, as the time required the output voltage to rise to 90% of its final value. It depends on the load resistance and capacitors. Faster rise time makes certain that no delay occurs in the system during the producing of a stable output voltage. Lastly, the achieved DC voltage at the output contains some undesired ripple or noise, which is related the load current. To smooth the DC output voltage for supplying the system, a large capacitor is required [6] [12] [17].

The main electrical component to convert the RF signal to DC voltage is a diode. The saturation current, junction capacitance and conduction resistance of the diode have mainly effect on the performance of the rectification. The most attractive candidate for rectifier circuitry is a silicon Schottky barrier diode. This type of diodes is suitable for rectifying due to low forward voltage and lower junction capacitance than PN junction diodes. As previously stated, the low threshold voltage causes higher efficiency at low powers, and the maximum operating frequency of diode improves because of the low junction capacitance [1] [12].

The most common method for the rectifier circuitry is the diode-based approach. The basic form of a rectifier consists of a diode, which is connected in series to a load, and a capacitor to smooth ripples of the output voltage. This kind of the rectifier structure, as can be seen in Figure 3. (a), is called a single-stage rectifier and it is introduced in two different topology as half-wave and full-wave rectifying.

A charge pump is a number of diodes connected in series to rectify the RF input signal and obtain the higher output DC voltage using the particular characteristics of diode in rectifying the distinct levels of the signal. The simplest approach of charge pump, a voltage doubler, includes two diodes (usually Schottky diodes) and two capacitors, as shown in Figure 3. (b). Although, the input capacitor is employed to prevent flowing DC current from the antenna to the diodes, it stores charge and hence, the currents of high frequency are allowed to flow. In addition, accumulating the resulting charge to smooth the output voltage is the task of the output (second) capacitor. When the RF input signal is in the negative half cycle and higher than the forward voltage, the first diode is turned on, and the input capacitor is charged up to the maximum value of the input signal by flowing the current from the ground through the diode. At the positive half cycle, the output diode is in the forward biased and the first diode is turned off. In this case, the output capacitor is not only charged through the output diode but also the charge stored in the input capacitor is transferred to the output capacitor. Thus, the output voltage (V_{DD}) is twice of the peak voltage of the RF input source (V_{peak}) subtracting the threshold voltage of the diode (V_{TH}) [18].

$$V_{DD} = V_{peak} + (V_{peak} - V_{TH}) - V_{TH} = 2(V_{peak} - V_{TH}) \tag{2.13}$$

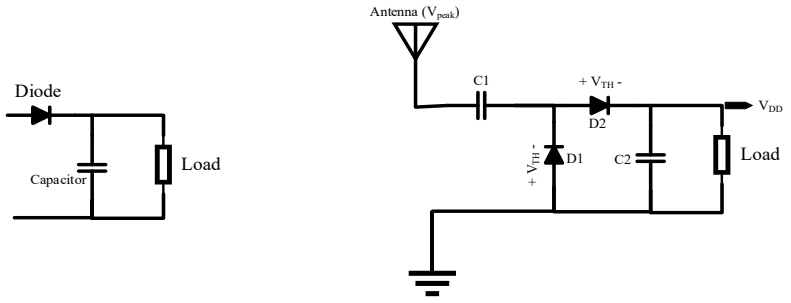

(a) *(b)*

Figure 3. *(a) The schematic of a single-stage rectifier (b)) The schematic of a voltage doubler [18]*

Stepping up the output voltage to the utilizable levels is one of the superiority of charge pumps, which can be provided by cascading diode-capacitor stages to form a voltage multiplier. In this case, by ignoring the noise of the previous stage, the output voltage for N stage can be calculated by [18],

$$V_{DD} = 2N(V_{peak} - V_{TH}) \tag{2.14}$$

Villard voltage multiplier and Dickson charge pump rectifier are commonly topologies used in integrated applications, as illustrated in Figure 4 and Figure 5, respectively. As is obvious, both topologies configured with voltage doubler cells in several numbers of stages. The only difference between the Villard and Dickson charge pumps configuration is that the Villard structure is formed by voltage doublers connected in series and the Dickson multiplier is organized by voltage doublers connected in parallel. Although, increasing the number of stages to enhance the output voltage leads to enhance the power losses and hence, the total efficiency will be decreased. It is one of the best structure to achieve higher output DC voltage for the RF energy harvesting applications [6] [17].

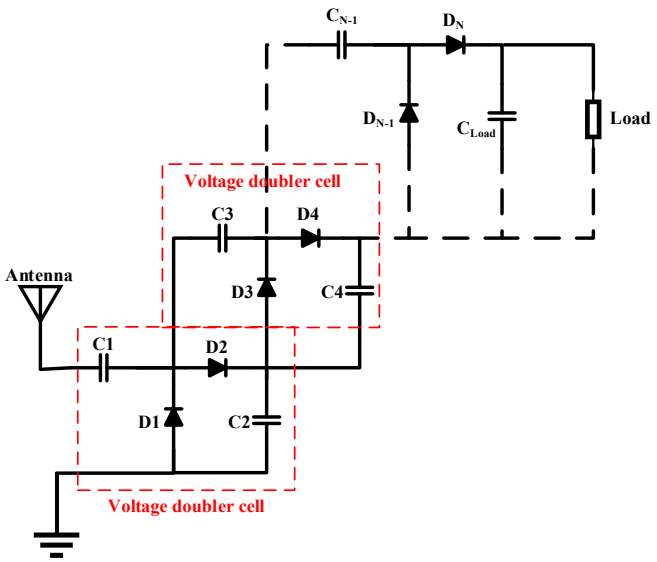

Figure 4. *Villard voltage multiplier [12]*

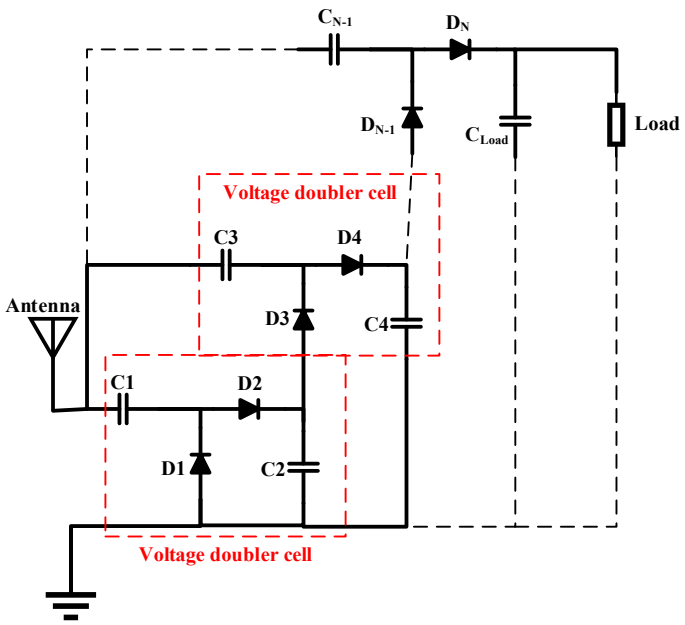

Figure 5. *Dickson charge pump [12]*

2.5 Energy Storage

The last block of the energy harvesting system is referred to the energy storage. A capacitor or a rechargeable battery is used as an energy storage unit. This unit should store all converted RF signal for future use. The Villard or Dickson charge pumps topologies used for the rectifier contain a capacitor in parallel with the load at the last stage. As discussed previously, it is utilized to smooth the produced constant output voltage. This last capacitor can be introduced as the storage unit. In order to choose the suitable component for this unit, various types of energy storage components along with their main features are studied. Moreover, the advantages, disadvantages, and applications of each of them are described in detailed to make a decision for using one of them as energy storage in this work.

2.5.1 Supercapacitors

Electrochemical double-layer capacitors (EDLC), also known as supercapacitors or ulteracapacitors, are a new technology, which stores the electrical energy in an electrolytic double-layer, thus provide an availability of new power electronics and industrial storage. These capacitors have a higher energy storage density simultaneously with a higher power density compared to the conventional electrolytic capacitors. Besides, there are two main features, which make supercapacitors more preferable tool than conventional batteries for short-term energy storage in power electronics. First, they have extremely high capacitance values, many thousand farads, and second, they are able to charge and discharge very fast due to low inner resistance [19].

A supercapacitor consists of a separator, an electrolyte, and two electrodes, which made up electrochemical materials with the highest specific surface area. The electrochemical materials are used to form a double layer with a maximum number of electrolyte ions, which leads to the effective separation of charge. Since the capacitance is proportional to the surface area, the porosity of these materials, which provide a larger surface area into a given volume, resulting in much greater capacitances than conventional capacitors. In brief, ECLD is one the most prominent energy storage with tremendous applications due to its properties including high ionic electrolyte conductance, high ionic separator conductance, high electronic separator resistance, high electrode conductance, high electrode surface, low separator and electrodes thickness. Therefore, they are suitable energy storage devices for vehicles and energy harvesting systems. Moreover, supercapacitors are also growing in popularity as fast charging tools in computer systems, power conditioners, cameras, power generators, and solar energy systems [19].

Because of these properties, EDLCs have several advantages containing durability, high reliability, and no maintenance. Besides, supercapacitors have a long lifetime, which reaches one million cycles without any degradation, and operate over a wide range of temperature and in diverse environments. Thus, they are environmentally friendly due to

their long lifetime in addition to recycling or neutralizing easily. The efficiency is typically around 90% because of extremely low equivalent series resistance (ESR). As above-mentioned, they can reach very high rates of charge-discharge cycles with discharge times in the range of seconds to hours and high power density, which is about ten times greater than that of conventional batteries[19].

On the other hand, supercapacitors show some disadvantages including the higher self-discharge rather than electrostatic capacitors and also lower absorption rather than dielectric absorption of any type of capacitors [19].

2.5.2 Lithium-Ion Batteries

A lithium-ion battery, also called Li-ion battery or LIB, is a rechargeable battery with high energy density, thus it has become the most important storage technology in the areas of portable and mobile applications. A lithium-ion battery consists of an anode, cathode, separator, electrolyte, and two negative and positive electrodes, which are made up lithium-ion electrochemical cells as the electrode materials instead of metallic lithium. The electrochemical cells of the electrodes release lithium ions from the anode to the cathode and vice versa, depending on the direction of the current flow. Furthermore, one of the most eminent factors of a lithium-ion battery is its highest energy density for weight due to the greatest electrochemical potential and the lightest weight of these metals. Lithium-ion batteries are very flexible and universal storage devices, which are fabricated from different materials along with various design, therefore, they are made in wide variety of shapes and sizes. The efficiency of lithium-ion batteries are very high, approximately in the range of 95%-98% due to an internal resistance of the cells. In addition, lithium-ion is a low maintenance battery with no memory and no scheduled cycling which is required to prolong the battery's life. The self-discharge in this battery is relatively low around 5-10% per month, which is less than half compared to nickel-cadmium. The most significant advantages of lithium-ion batteries are the high energy density and high open circuit voltage, which means that greater power can be supplied at a lower current. Lithium-ion is environmentally safe and causes little harm when disposed of. As a result, it can be used in many branches ranging from military and aerospace to electric vehicle and smart cellphones [20].

Despite its overall advantages, a lithium-ion battery has some disadvantages like its higher cost to manufacture, about 40% more than nickel-cadmium. Subject to aging, the cell’s capacity, and thus its life reduces over time. Also, this loss increases by high charge levels and at high temperatures, therefore manufacturers recommend storage temperatures of 15°C (59°F). The voltage and current of a lithium-ion battery circuit need to keep within safe limits and should be avoided over-charging and over-discharging due to its high internal resistance [20].

2.5.3 Lithium-Polymer Batteries

A lithium-ion polymer battery, also called polymer lithium ion or LIP, is a rechargeable battery with similar technologically as an organic solvent included and differentiates only in the type of electrolyte used. Indeed, the electrolyte LIP is soaked in a solid polymer composite instead of an organic solvent in an organic solvent. Lithium-ion polymer batteries have more flexible shape and size than LIB due to the simplification of the polymer according to its fabrication, ruggedness, safety and thin-profile geometry. However, there are some drawbacks because of the poor conductivity of lithium-polymer which results in too high internal resistance and incapability to deliver the current bursts. Hence, in order to increase the conductivity, the temperature of the cells has to increase over 60 degrees, which makes them inappropriate storage tools for portable applications. Whereas, the added volume of electrolyte provides increased energy storage and this makes them ideal for use in high capacity low power applications such as in radio controlled equipment, personal electronics, and electric vehicles [20].

In brief, lithium-ion polymer batteries are reputed because of very thin geometries, which feasible in the profile of a credit card, flexible form and high safety due to overcharging resistant and less electrolyte leakage. Although, lower energy density, which decreases cycle, count and increases the cost to energy ratio compared to lithium-ion, makes it less applicable storage tool [20].

2.5.4 Solid State Batteries

A solid-state battery is a battery based on lithium-ion technology but using solid electrodes and solid electrolytes with a thin layer of non-flammable material instead of liquid electrolyte. These solid materials have a high ionic conductivity, which reduces the internal resistance of the battery. Solid-state batteries is a very new technology with low-power density and high-energy density, which makes them ideal for use in electric vehicles. These batteries eliminate the difficulties of solid-solid interfaces, for example, they can be fabricated in thin film form. In short, it is significantly beneficial to develop solid-state batteries for storage industries due to no changes in performance with temperature, no electrolyte leakage, long shelf lives, and high power-to-weight ratio [20].

Consequently, the supercapacitor is the best choice for this work due to high rate of charging and discharging with discharge times in the range of seconds, extremely low equivalent series resistance (ESR) and its lifetime, which is one the important aim in using an RF energy harvesting system.

3. BASIC THEORY OF AN RF SWITCH

3.1 RF Switch

In a general definition, a component that is able to open, close or change the connections in an electrical circuit, is called switch. A switch shows different resistance values in ON or OFF states to flow the current into the circuit. An ideal switch represents infinite resistance value during the OFF state and zero value for resistance in ON state. Nevertheless, in practical, during the ON state, the resistance exhibited is not completely zero; it contains a certain value, and in the OFF state, it exhibits a finite resistance value [21].

RF switches are able to create multiple transmission paths for high frequency signals. To attain the desired performance of RF electronics devices, various technologies and topologies have been considered. Two standard categories of RF switches, which are used recently, include electromechanical and solid state switches [22].

Electromechanical Switch

Electromechanical term is referred to devices that contain mechanical movement parts to provide an electrical signal or an electrical signal to make a mechanical motion such as relays which consists of a number of contact mechanical switches to isolate the circuit by controlling the voltage or current. Although, this kind of switch was extensively used previously, the micro-electromechanical-systems (MEMS) switch technology recently is an attractive technology for switches to improve the reliability and quality packaging [22].

Solid State Switch

Electronics devices that do not comprise any vacuum tubes or mechanical devices introduced as solid state components. Indeed, solid state term explains electronics devices which contain unheated solid semiconductor materials such as Silicon or Germanium for flowing electrons.

Solid state switch also is defined as a component without any moving parts. Hence, there is no mechanical erosion. In addition, it can resist properly to the shock, vibration and mechanical wear. Therefore, it is more reliable and includes much longer life than the electromechanical switches. One of the drawbacks of the solid state switch includes the higher insertion loss due to its inherently ON resistance.

Consequently, the solid state switches are mostly employed in the circuits, where the most significant aim of designing is the fast switching and long operating life [22].

Three main types of solid state switches are categorized by [22]:

- PIN diode switches
- Field-effect transistor (FET)-based switches
- Hybrid(FET and PIN diode) switches

In order to choose the suitable component for the RF switch, various types of solid state switches along with their advantages and disadvantages are studied. After that, the best candidate is chosen and discussed about its features and configurations.

3.1.1 PIN Diodes

The PIN diode is a semiconductor component that is widely used as a variable resistor at RF, UHF and microwave frequencies. Unlike the varactor diodes, which are known as the voltage-controlled capacitors, a PIN diode is defined as the bias current- controlled device. Varying the resistance value of the PIN diode depends on the bias current flowing through the diode. Thus, this value, which is changed from less than 1 Ω to more than 10 kΩ, can be determined by the forward bias state of the diode. PIN diode is typically employed for the switching. Especially, the PIN diode is able to control high RF powers when lower DC levels are used [22].

3.1.2 FET Switches

The FET-based switch is a semiconductor transistor that controls the device electrical behavior by using an electric field. The voltage that is applied between the gate and source can control the current that flows between the drain and source terminals. As the drain-to-source resistance can be controlled accurately, FET switches are known as stable switches [22].

FET switches have a good isolation at low frequencies but at high frequencies, the capacitor placed between the drain and source will affect the isolation and reduce it. Moreover, FETs can be involved a simpler DC biasing path because the RF path and biasing path of the switches are not connected to each other. Hence, it does not need to use an expensive RF choke for high quality performances. In spite of the ability of FETs to eliminate the RF chokes requirement, they contain high ON resistance, which results in the higher insertion loss at high frequencies [22].

3.1.3 Hybrid (FET and PIN Diode) Switches

Two important specifications of PIN diodes and FET switches include frequency range and isolation, which cannot meet needs for their applications at the same time. Therefore, a new series of switches can be produced by combing the PIN diode and FET technologies that is called hybrid switches [22].

The utilized topology for hybrid switches consists of shunt PIN diodes and series FETs. Shunt PIN diodes are applied to provide a specified amount of current to improve the isolation at high frequencies and FETs are employed to increase the bandwidth from lower frequencies with great isolation. The only disadvantage of this topology is the non-convergence between the RF path and biasing path that DC biasing path may experience some RF leakage [22].

Consequently, among all types of RF switches, PIN diodes are the best choice to use in broadband switch design at high frequencies, due to the high speed switching, low package parasitic components, low resistance of forward-bias, and small physical size compared to the wavelength of the signal. Therefore, PIN diode was used as an RF switch in this work. The PIN diode functional and its specifications will be described in details in the next sections [22].

3.2 PIN Diode Principles

An intrinsic "I" layer with a high resistivity material is used to form the structure of a silicon semiconductor diode called PIN diode. This layer is sandwiched between two other regions, a P-type, and an N-type region, as displayed in Figure 6. (a).

When the PIN diode is forward biased, the charge carriers from P-type and N-type regions are injected into the "I" layer. Storing a finite amount of charge exhibits the diode as a very small resistor (R_s) that is in series with a parasitic inductance (L). In this case, the resistor can pass the RF signal with a very low insertion loss. In addition, the PIN diode attains an excellent isolation due to the inverse ratio of the forward bias current and resistance. Depleting of any charge carriers from the "I" layer at the reverse or zero bias leads to appear the diode as a very high resistance (R_P) in parallel with a small capacitance (C_T) and the parasitic inductance in series. This capacitance consists the parasitic capacitance (C_p) and the junction capacitance (C_J). In this state, a small capacitor helps to block the RF signal and hence, the performance of the diode will be improved at high frequencies. The equivalent circuits of the PIN diode at forward and reverse bias are shown in Figure 6. (b) and Figure 6. (c), respectively [22] [23].

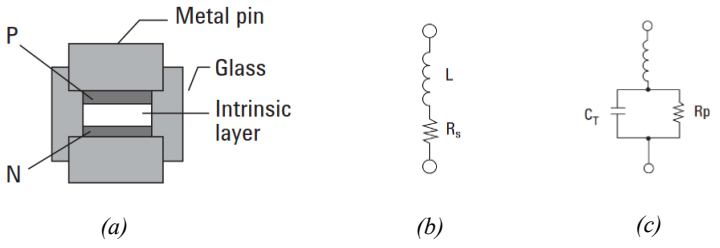

Figure 6. *(a) Cross section of a basic PIN diode (b) The equivalent circuit of the PIN diode at Forward bias (c) at Reverse bias [22]*

In general, various geometries of PIN diodes can be achieved by changing the width of "I" region and the area of diode, which leads to having similar characteristics of the R_s and C_T and other small signal specifications. Nevertheless, the thicker "I" layer results in creating larger breakdown voltage and better distortion characteristics. On the other side, the thinner region makes a device with much higher switching speed [23].

3.2.1 The PIN Diode Switches Models at Low Frequency

Forward Bias

According to the definition of the PIN diode, it is a suitable device for high frequency applications. Indeed, it contains a limitation in operating at lower frequencies. The resistive performance of the component can be obtained by the quantity of the charge stored in the "I" region, operating frequency and non-bias signal value applied to the PIN diode. Hence, the behavior of the PIN diode can be determined by the frequency of the non-bias signal, which is higher or lower than the transit time frequency. The transit time frequency is expressed by [24],

$$f_t = \frac{1}{2\pi\tau} \tag{3.1}$$

where τ is the carrier lifetime. Additionally, the frequency of transit time can be calculated as a function of the "I" region width as follow [24],

$$f_t = \frac{1300}{W^2} \tag{3.2}$$

where W is the width of the "I" region. If the operating frequencies are larger than the transit time frequency, then the resistance appeared at the forward bias is dependent on the inverse ratio of the quantity of stored charge (Q) as calculated by [24],

$$R_s(\Omega) = \frac{W^2}{(\mu_P - \mu_N)\mathrm{Q}} \tag{3.3}$$

where μ_P is the hole mobility and μ_N is the electron mobility, and stored charge (Q) can be given by,

$$\mathrm{Q} = I_f\tau \tag{3.4}$$

where I_f is the forward current [22].

When the frequencies are smaller than the transit time frequency (f_t), the PIN diode operates as a Silicon PN junction semiconductor diode and rectifies the RF incoming signal. Thus, the PIN diode is not appropriate for employing at low frequencies as a switch. The range of transit time frequency is typically between a few KHz and 1 MHz [22].

Reverse or Zero Bias

As stated in 3.1 section, a low capacitance in parallel with a high resistor comprise the RF electrical model of the PIN diode at the reverse bias. The low capacitance is appeared due to remaining some carrier charges in a small portion of the "I" region, called as un-depleted portion. The applied reverse bias level and the signal frequency through the PIN diode have the effect on the reverse resistance and capacitance values [24].

The reactance of the undepleted layer is higher than its resistance value at low frequencies. By enhancing the frequency, the undepleted region reactance is reduced and hence, the overall reverse capacitance of the diode will be declined. As a result, the dielectric relaxation frequency is defined as the frequency at which the reactance of the undepleted layer is equal to the resistance value. This frequency can be given by [22][24],

$$f_d = \frac{1}{2\pi\rho\varepsilon} \tag{3.5}$$

where ρ is the resistivity of "I" region and ε is the dielectric constant of "I" region material.

Therefore, the PIN diode operation is like a varactor diode at a much lower frequency than the dielectric relaxation frequency (f_d). At the frequencies above the f_d , the total capacitance C_T comprising of the parasitic capacitance (C_p) and the junction capacitance (C_J) is calculated by [22],

$$C_J = \frac{\varepsilon A}{W} \tag{3.6}$$

where A is the area of diode junction.

As a result, PIN diode limits operation at low frequencies and cannot act as a useful switch [22].

3.3 PIN Diode Switch Design

As discussed in previous sections, the specifications of the PIN diode in forward and reverse bias can be considered as a criterion for designing a switch at RF frequencies. Obviously, the PIN diode exhibits a very low impedance in forward bias and a high impedance in reverse bias condition at lower microwave frequencies, e.g. lower than 2 GHz [21].

To achieve the proper switch performance, considering the reflection characteristics is more important than power dissipation. Naturally, the diode dissipates a very small amount of energy itself and, as will be explained below, the PIN diode switch circuits act like filter devices in many designing. Thus, the losses are on the second priority [21].

3.3.1 The Fundamental Parameters for PIN Diode Switches Designing

Isolation

Isolation measures the RF power that is not transmitted to the load through the switch when it is in the OFF state. This power can be included both attenuation and reflection loss. On the other words, isolation is defined as the difference between the output power level when the path of the switch is ON and the level of output power measured when the switch is in OFF state. The equation (13) presents the isolation calculation [21] [22].

$$Isolation\ (dB) = (P_{out})_{ON}(dBm) - (P_{out})_{OFF}(dBm) \tag{3.7}$$

However, the PIN diode switches include the transmission loss in both ON and OFF states, any problems including transmission loss through the physical structure will be prevented with the equation (3.7). Truly, PIN diode switches have excellent isolation performance at RF frequencies, which can avoid any leakage signal into the desired signal path. But PIN diodes offer poor isolation at lower frequencies below 100 MHz, due to its limitation at low frequencies [21][22].

Insertion Loss

Ideally, all incident signal power should be passed through the switch but in reality, all incident energy will not be absorbed by the switch and some amount of this signal is reflected when the PIN diode switch is in the ON state. The amount of this amplitude reduction is called as insertion loss. As another definition, insertion loss is the signal power loss in the ON state of the switch, which is typically defined in terms of the decibel (dB) [25].

PIN diode switch contains a significant performance of the insertion loss at higher frequencies. However, due to leaking the RF signal into the DC biasing path, PIN diode experiences high insertion loss at lower frequencies. Thus, insertion loss is an important parameter that should be considered in PIN diode switch designing [22].

Switching Speed

The minimum time required for changing the switch state is known as switching speed. The most common characteristics to define the switching time involve rise time, fall time, ON time and OFF time, as shown in Figure 7. Switching speed is dependent on the driver circuit and the characteristics of the switch, as well [22].

Rise time refers to the time for raising the RF signal from 10% to 90% of the final level during the switch changes from OFF state to ON state. Fall time is the required time that RF signal declines from 90% to 10% of the initial value when the switch starts to change the state from ON to OFF. ON time is the duration that takes from 50% of the control

signal transition to 90% of the RF output detection during the changing switch state from OFF to ON. The OFF time is related to the necessary time for dropping the signal control transition from 50% to 10% of the RF output detection when the switch change from ON to OFF state [22].

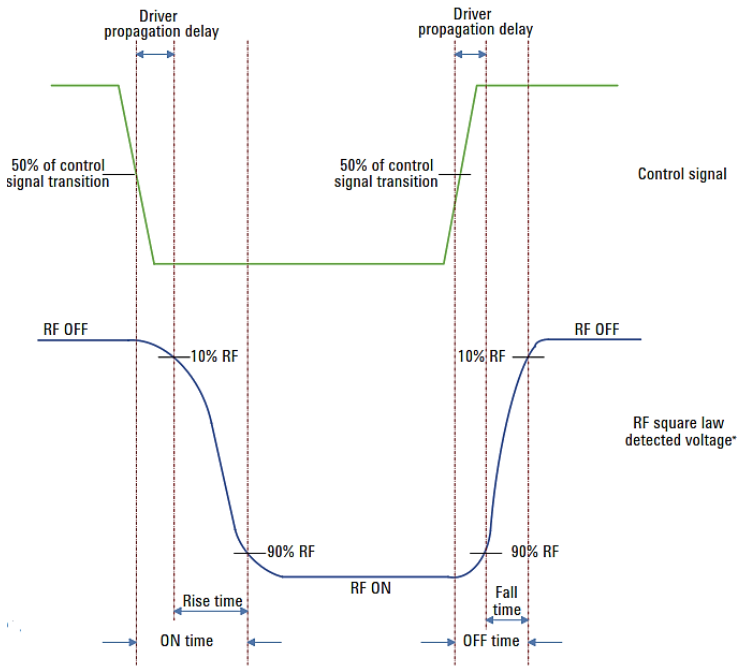

Figure 7. *Switching time definition of a switch [22]*

PIN diode includes short time performance to reach rise and fall time, which is about tens of nanoseconds and it contains fast switching time (ON/OFF). The ON and OFF time takes about tens to hundreds of nanoseconds [22]. The switching speed of the PIN diode can be calculated by,

$$T_{FR} = \tau \, log_e \left(1 + \frac{I_F}{I_R}\right) \tag{3.8}$$

where T_{FR} is the switching time from forward to reverse bias, τ is the carrier lifetime, I_F is forward current and I_R is the reverse current. The switching time from reverse bias to forward bias depends on the width of the "I" layer, W. By decreasing the width, the switch will be faster [22].

3.3.2 PIN Diode Switch Design Configurations

In this subsequence section, the two basic configuration types of the PIN diode switch as a common component for controlling the RF signal are described. All structures of the switch are considered as a symmetrical linear two-port network and its parameters such as input power source impedance (Z_S), load impedance (Z_L) and all transmission lines are assumed 50 Ohms [21].

Single Pole Single Throw Switches (SPST)

Series SPST Switch

Figure 8 demonstrates one of the basic types of PIN diode series SPST switch. The series structure of the diode can be used in the broad frequency range when the insertion loss should be at the minimum level. In this configuration, when the PIN diode is in forward biased, all incident power pass and exhibits a certain amount of ON resistance between the RF power source and load. Under the zero or reverse bias condition, PIN diode presents a high impedance between the RF source and the load and does not pass the RF signal through the load. In the series configuration of the switch, the isolation will be the maximum value as a function of the PIN diode's capacitance. In this case, the forward biased resistance of the diode has an effect on the value of the insertion loss and power dissipation [21] [25].

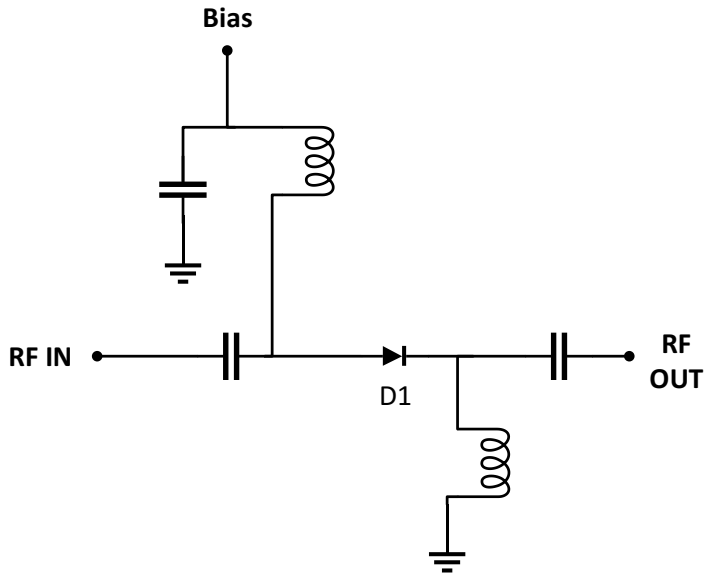

Figure 8. *Series SPST switch [21]*

Shunt SPST Switch

Figure 9 illustrates the other basic types of PIN diode shunt SPST switch. In contrast, the series connected switch, the shunt structure determines the high isolation for broadband designs. Since no switch elements are placed in series with the transmission lines, the insertion loss has a low value. In addition, in the shunt designs, the insertion loss is the function of the PIN diode's capacitance, while, the ON resistance of the diode has an effect on the isolation and power dissipation characteristics [21][25].

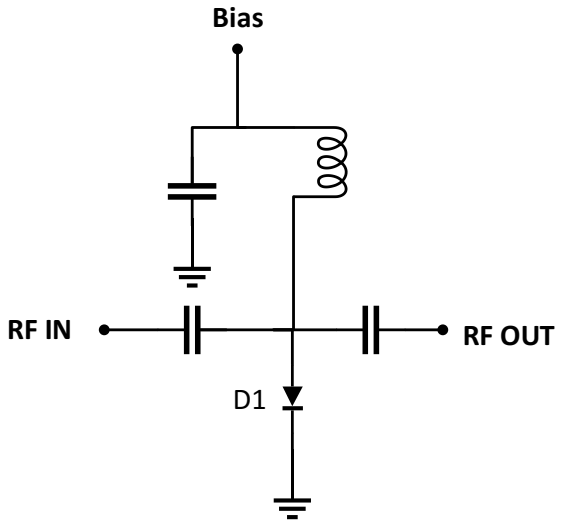

Figure 9. *Shunt SPST switch [21]*

Single Pole Double Throw Switches (SPDT)

Single Pole Double Throw switch is the simplest model of the Single Pole Multi-throw switch configuration. In this structure, the RF input power applied into a single input path can be injected in either of two transmission lines at the output. Figure 10. (a) and Figure 10. (b) show the series SPDT and shunt SPDT switches, respectively [21].

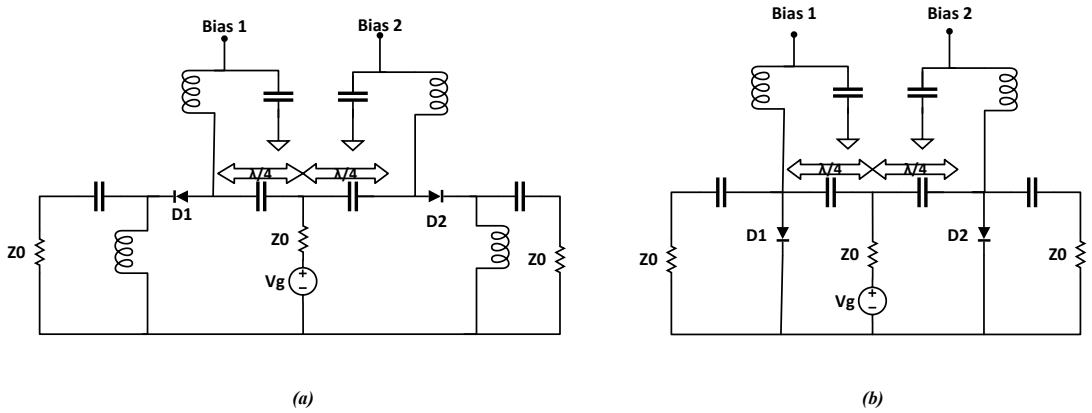

Figure 10. *(a) Series SPDT switch (b) Shunt SPDT switch [21]*

If the SPDT switch is configured symmetrically, the performance of each switching branch resembles the performance of the equivalent SPST switches. The difference is about the multi-throw switch isolation, which is enhanced by 6 dB. Because, when one of the branches is OFF, it will be shunted with the ON branch and its termination of 50 Ohms, which results in decreasing the RF voltage across the OFF diode by 50% less than the same case in the SPST switch [21].

Designing the shunt SPDT switch structure including the quarter-wavelength transmission lines placing between the RF power source and the PIN diodes, can increase the

electrical performance. In this case, because of the multi-throw junction effect, the isolation will be enhanced two times approximately [21].

Multi-Throw Switches

The other type of multi-throw switches includes two quarter-wavelength transmission lines in cascading with terminated by a shunt diode in each section. This structure is a band-limited configuration, as shown in Figure 11. This switch design can produce high input impedance at the RF common port in the OFF branch to avoid load impedance of the ON branch. In spite of achieving very high isolation, the bandwidth is limited and the insertion loss will be enhanced using added shunt PIN diodes and transmission lines as sections. Besides, at RF or high frequencies, cross-coupling between the elements of a switch makes the isolation limits, which leads to signal feed-through directly between the input and output [21].

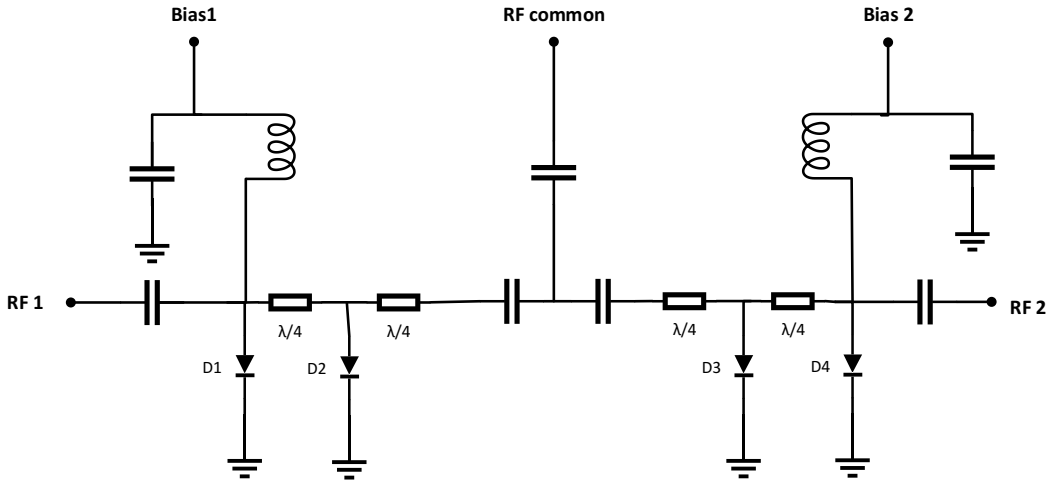

Figure 11. *Band-limited shunt Multi-throw switch [21]*

Compound Switches

To improve the performance of the switch, a combination of series and shunt PIN diodes is configured, that is called compound switch. Compound switches can overcome the difficulty of achieving the much higher isolation than it is attained by a single configuration of a PIN diode, in either series or shunt structure at high frequencies [23].

The most popular configuration of compound switches are series-shunt SPST switch and TEE compound switches, as displayed in Figure 12. (a) and Figure 12. (b), respectively. To determine the insertion loss of the compound switches, the series diode should act in forward bias, while the shunt diode is under the reverse or zero bias. Although this kind of switches can improve the overall performance, the complexity of the switches leads to make a degradation in the insertion loss [21] [25].

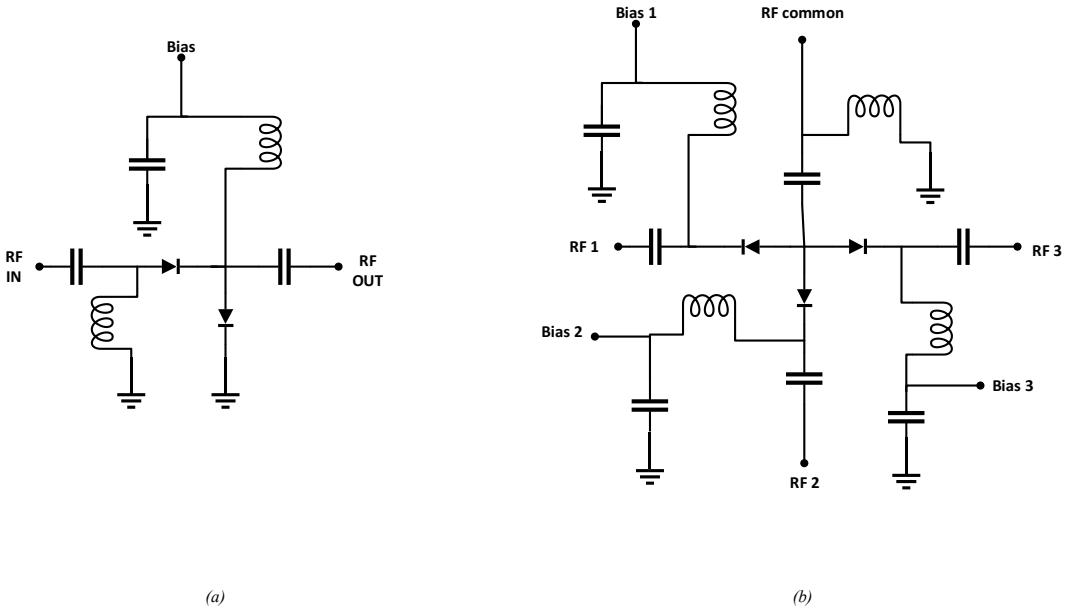

Figure 12. *(a) Series-shunt SPST switch (b) TEE compound switches [21]*

Finally, the overall performance of the series, shunt SPST, and compound switches is summarized in table 1.

Table 1. *Summary of formulas for SPST switches [21].*

Type	Isolation (dB)	Insertion Loss (dB)
Series	$10\log_{10}\left[1+\frac{1}{(4\pi f C_T Z_0)^2}\right]$	$20\log_{10}\left[1+\frac{R_S}{2Z_0}\right]$
Shunt	$20\log_{10}\left[1+\frac{Z_0}{2R_S}\right]$	$10\log_{10}[1+(\pi f C_T Z_0)^2]$
Series-Shunt	$10\log_{10}\left[\left(1+\frac{Z_0}{2R_S}\right)^2+\frac{1}{4\pi f C_T Z_0}\left(1+\frac{Z_0}{2R_S}\right)^2\right]$	$10\log_{10}\left[\left(1+\frac{R_S}{2Z_0}\right)^2+(\pi f C_T)^2(Z_0+R_S)^2\right]$
TEE	$10\log_{10}\left[1+\frac{1}{(2\pi f C_T Z_0)}^2\right]$ $+10\log_{10}\left[\left(1+\frac{Z_0}{2R_S}\right)^2+\left(\frac{1}{4\pi f C_T R_S}\right)^2\right]$	$20\log_{10}\left[\left(1+\frac{R_S}{2Z_0}\right)^2\right]$ $+10\log_{10}[1+(\pi f C_T)^2(Z_0+R_S)^2]$

4. FUNDAMENTALS OF ANTENNAS AND RFID

4.1 Electromagnetic Theory

In a general definition, an antenna makes guided waves in a form of transition on a transition lines into free space waves and vice versa in the receiving form. The official IEEE definition of an antenna refers to “That part of a transmitting or receiving system that is designed to radiate or receive electromagnetic waves”. Indeed, most antennas act as reciprocal components. It means that they can receive or transmit the signal with the same behavior. Thus, antenna as a crucial device can transfer information between two different locations without any interference at different electromagnetic spectrum. Antenna must be used in various applications such as mobile communications, broadcasting, or even in non-communication systems involving remote sensing and industrial applications, hence, it is essential to study the electromagnetic theory as the key concept of antenna theory and wave propagation [26].

4.1.1 Maxwell Equations

The basics of theoretical for antennas are introduced by the Maxwell’s equations. Four single equations comprise Maxwell equations, which describe the relation among magnetic field, electric field, electric current and electric charge. Basically, these equations say how electric and magnetic fields are generated and specify their effects on each other. In addition, the effects of the current and charges on these fields can be studied by the equations. The fundamental law known as induction Faraday’s law (4.1), Ampere’s circuital law (4.2), Gauss’s law for electric fields (4.3) and Gauss’s law for magnetic fields (4.4) are used to define these four equations [15],

$$\nabla \times E = -\frac{\partial B}{\partial t} - M \tag{4.1}$$

$$\nabla \times H = \frac{\partial D}{\partial t} + J \tag{4.2}$$

$$\nabla . D = \rho \tag{4.3}$$

$$\nabla . B = 0 \tag{4.4}$$

To calculate the current density J in equation (4.2), equation (4.5) will be applied,

$$J = \sigma E \tag{4.5}$$

Where σ denotes the conductivity of the material [15].

4.1.2 Electromagnetic Radiation

Two different models involving the wave model and particle model can describe the electromagnetic radiation. In the wave model, electromagnetic waves (EM) is referred to the electric and magnetic fields. In this viewpoint, electromagnetic radiation is defined as a form of electromagnetic waves at which these two fields oscillate at the same time in planes, which are perpendicular to each other and to the propagation direction through free space. In fact, the perpendicular of EM fields to the direction of energy and wave propagation is called transverse wave. The characteristics of the electromagnetic position in the EM spectrum is dependent on the oscillation frequency or wavelength. Hence, the EM spectrum contains various operating frequency bands [26].

In the particle model, electromagnetic waves can be created by accelerating the charged particles; also, the produced EM waves can be interacted by other charged particles. EM waves take away the energy; momentum and angular momentum belong to the particles of the source and convey them to the interacted substance by them. Electromagnetic radiation depends on the EM waves, where radiate independent of the charges movements. In this state, the EM waves are sufficiently far away from the charged particles; hence, Electromagnetic radiation can be introduced as the far field. As a result, if the charged particles are close to the EM fields, these files are defined as the near field [26].

4.1.3 Permittivity and Permeability

Permittivity is a measure of how much a medium can polarize in response to the external electric field, thus it is determined by the stored and dissipated energy inside the medium as follows [27],

$$\varepsilon = \varepsilon' - j\varepsilon'' \tag{4.6}$$

where the real part of permittivity, ε', is the stored energy which represents the relative permittivity (static dielectric contribution) and imaginary part of the permittivity, ε", express the dissipated energy in a dielectric medium. Moreover, the loss tangent, which represents the inherent dissipation of the medium, is the ratio (or angle in a complex plane) of the reaction of lossy materials to the electric field E in Maxwell's curl equation to the lossless reaction. In general, the loss tangent can be calculated as [27],

$$tan\,\delta_e = \frac{\sigma_e}{\omega\varepsilon'} \tag{4.7}$$

where δe is known as the electric loss angle and σe is the effective conductivity which consists of two parts as written in equation (4.8) . The first part represents the static conductivity, which can be dominant owing to its large amount of free electrons and the second part shows the conductivity due to an applied alternating field, which is dominant along of the lack of free electrons [27],

$$\sigma_e = \sigma_s + \sigma_a \tag{4.8}$$

By substituting above equation into equation (4.7), the loss tangent is divided into two terms which relate to conductor with free electrons and response of dipoles inside dielectrics as follow,

$$tan\,\delta_e = \frac{\sigma_e}{\omega\varepsilon'} + \frac{\varepsilon''}{\varepsilon'} \tag{4.9}$$

where the first term results from the collisions of electrons. This term predominates in the conductor including more free electrons. The second term is related to the acceleration and deceleration when the dipole is rotated and when an applied electric field is changed, the dipoles inside dielectrics cannot instantaneously react [27].

Permeability is a measure of the ability to response a magnetic field inside of dielectrics, which is similarly can be obtained by the stored and dissipated energy inside the medium as follow [27],

$$\mu = \mu' - j\mu'' \tag{4.10}$$

where μ' and μ'' is the real and imaginary part of permeability, respectively. As carrying out similar analysis to the magnetic permeability, magnetic loss tangent same as electric loss tangent can be defined as [27],

$$tan\,\delta_m = \frac{\mu''}{\mu'} \tag{4.11}$$

Moreover, the magnetic flux inside the medium is proportional to the amount of external applied magnetic field as follow [27],

$$\bar{B} = \mu_0\,\mu_r\,\bar{H} \tag{4.12}$$

where μ_r is the relative permeability and μ_0 is the permeability of the free space.

4.1.4 Electromagnetic Plane Wave and Polarization

A plane wave is referred to the electric field (E field) (similarly for magnetic field (H field)), which is placed in the same direction, same value and same phase in the plane perpendicular to the propagation direction. This is known as a particular solution of Maxwell's equations. E and H fields are perpendicular to each other in an EM wave plane. Ideally, a basic wave plane propagates in a lossless medium where the complex propagation (γ) is purely imaginary and the real part of this constant (α) is zero. In reality, the medium is a lossy dielectric, which contains the conductivity (σ) equal to zero. In contrast, the medium permittivity (ε) is complex, hence, the $\alpha \neq 0$ and the amplitude reduces during the wave propagation. To express the dielectric medium loss, loss tangent ($tan\delta$) is employed, which is defined as the imaginary part of permittivity proportion to the real part.

When the used medium is a good conductor, then σ>>ωε and the wave magnitude keeps on reducing by the wave propagation in this type of medium. To define the loss of conductor, the skin depth or characteristic depth of penetration is used as given by,

$$\delta_s = \frac{1}{\alpha} = \sqrt{\frac{2}{\omega\mu\sigma}} \tag{4.13}$$

Where ω is the wave angular frequency. The EM wave cannot propagate inside the medium when the propagation medium is a perfect conductor [15].

The polarization of a plane wave, generally, defines the E field vector orientation in a fixed direction or may vary with time. The polarization of the EM wave is categorized into three types, linear, circular and elliptical polarizations. Similar to circular polarization, in elliptical polarization the vector of E field varies in two directions but with different magnitudes. In contrast with the linear polarization, circular polarization refers to vary the vector of E field in two directions with equal magnitude. The linear polarization refers to change the vector of E field in one plane, which can be in either x-plane or y-plane. Elliptical, circular and linear polarizations are demonstrated in Figure 13. (a), Figure 13. (b), and Figure 13. (c), respectively [28].

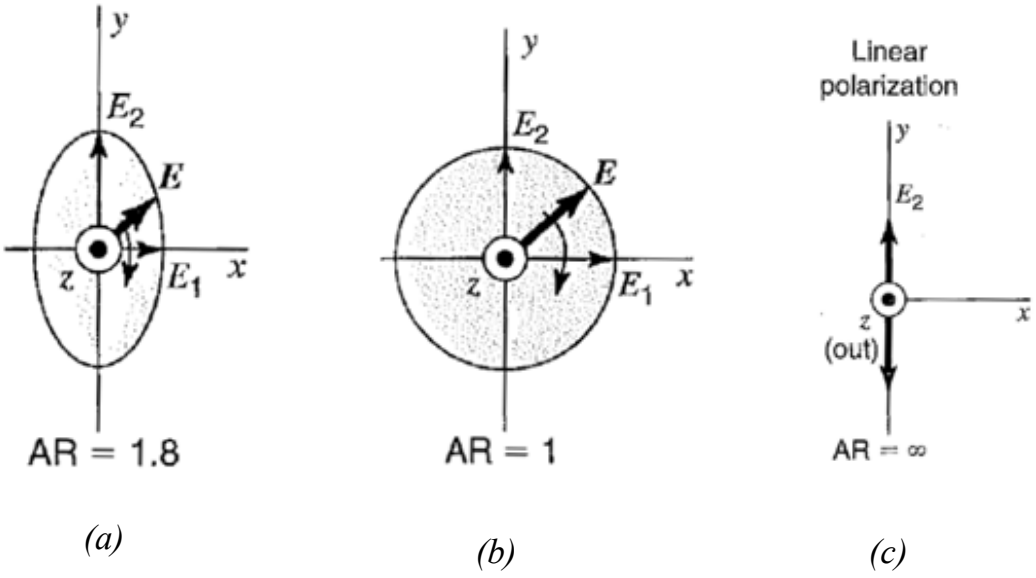

Figure 13. *(a) Elliptical polarization (b) Circular polarization (c) Linear polarization [28]*

The important parameter that explains the situation of the polarization is called axial ratio (AR), which is the proportion of the major field vector to the minor one. The value of this parameter in the linear polarization is infinity (∞). The value of AR parameter in circular polarization is 1 and In the elliptical polarization, the value of AR parameter depends on both vectors magnitude and it is between 1 to infinity (∞) [28].

4.2 Antenna Theory

An antenna can be known as a key component to understand electromagnetics and their wide variety of applications. The antenna is a passive component that captures and/or transmits radio waves. To characterize an antenna, different fundamental parameters should be recognized such as radiation pattern, gain, directivity, input impedance, return loss, bandwidth, polarization, half power beam width (HPBW), and axial ratio. Furthermore, antennas categorize as various models including wire antenna, aperture antenna, patch antenna, reflector antenna and lens antenna with different specific applications and performances [16].

4.2.1 Radiation Mechanism

According to the Maxwell's equations, a time-varying magnetic field, which is generated by the time-varying currents, can produce a time-varying electric filed simultaneously. Then, the two E field and H field, which are synchronized with time-varying, propagate at the speed of light in all directions. Since the E field and H field are perpendicular to each other and also perpendicular to the power and wave propagation direction, modifying current and more particularly the electric disturbance are introduced as a main factor of radiation. In fact, the amplitude or charge direction is changed [27]. Depending on the distance from the antenna, the characteristics of these two fields will be different. Considering this, the space around the antenna can be divided into three regions including reactive near field, radiating near field (Fresnel) and far field (Fraunhofer) [16].

The closest region to the antenna, where the reactive field is dominant, is called the reactive near field region. In general, the reactive near field is placed at a distance of $R < 0.62\sqrt{\frac{D^3}{\lambda}}$ from the surface of the antenna, where λ denotes the wavelength and D is the largest dimension of the antenna [16] [26]. The region where is between the reactive near field region and the far field region is defined as the radiating near field or Fresnel region. Radiation field is the dominant field in this region and the distribution of the angular field is varied by the distance from the antenna [16] [26].

The distance range of this region is $0.62\sqrt{\frac{D^3}{\lambda}} < R < \frac{2D^2}{\lambda}$ [24]. The most considerable region around the antenna is referred to the far field region where the radiation pattern of the antenna is necessarily not dependent on the distance from the antenna. In this region, a propagating wave can be considered as a plane wave. The distance to the far field begins at $R > \frac{2D^2}{\lambda}$ and broadens out to infinity distance. Figure 14 illustrates the field regions of an antenna [16] [26].

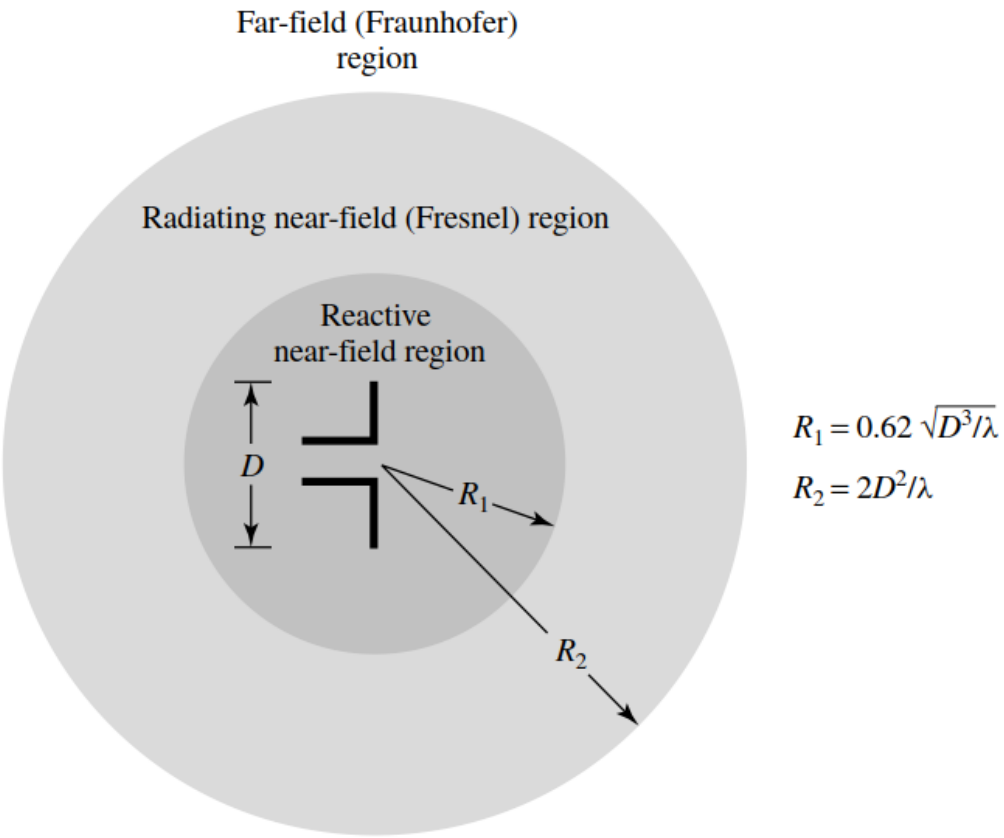

Figure 14. *The field regions of an antenna [16]*

4.2.2 Antenna parameters

Antennas include different parameters, which are essential to consider for proper designing of them. These all fundamental parameters are described in this section.

Radiation Pattern

The radiation pattern is a three-dimensional (3D) graphical display of the radiated power, which varies as a function of the direction away from the antenna. It is determined in the far field region of the antenna at a fixed radial distance from the antenna. The performance of the antenna can be explained in term of its main patterns including E plane and H plane. For a linearly polarization, the E-plane and the H-plane are described as the planes in the direction of maximum radiation from the antenna and parallel to the electric and magnetic field vectors, respectively.

As two planes are perpendicular to each other, a complete 3D radiation pattern is plotted at all angles of 'θ' and 'φ' in the spherical coordinate system and on the logarithmic scale or more commonly decibels (dB) [16]. Figure 15. (a) shows the E-plane and H-plane patterns for an aperture antenna and Figure 15. (b) demonstrate the coordinate system for analyzing the antenna.

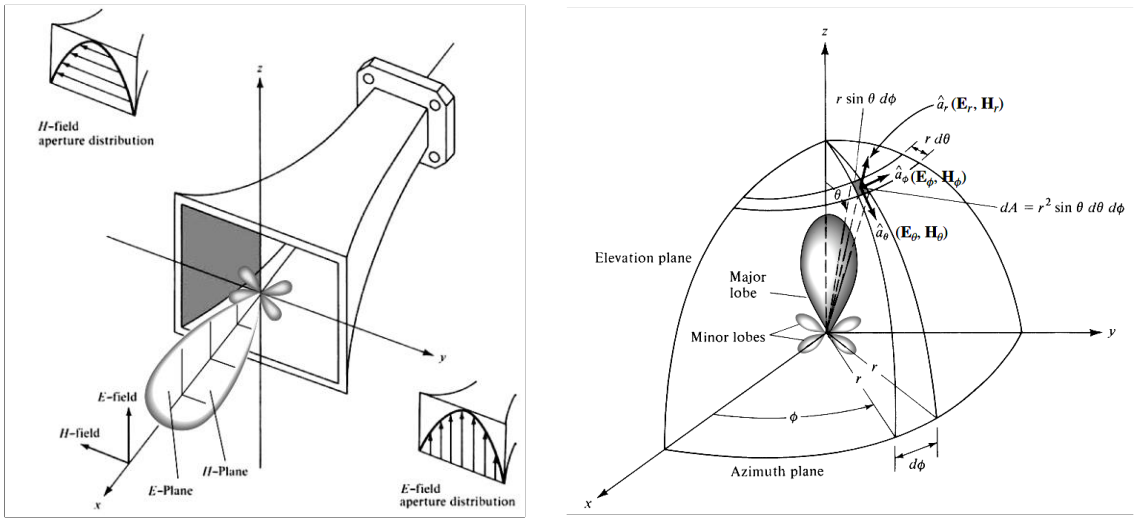

Figure 15. *(a) The E-plane and H-plane patterns for an aperture antenna (b) Coordinate system for antenna analysis[16]*

In addition, the radiation pattern can be divided into various parts that are called lobes. The portion of the radiation pattern, which is in the direction of the maximum radiation, is referred to the major or main lobe. Any other lobes except the major lobe are known as the minor lobes, which comprise of side lobes and back lobes. Side lobes are close to the major lobe with smaller beams. Truly, side lobes are usually radiation in undesired directions. Back lobes are in the opposite direction of the major lobe with the angle of 180˚. Figure 16 displays the radiation pattern of an antenna with different lobes [16].

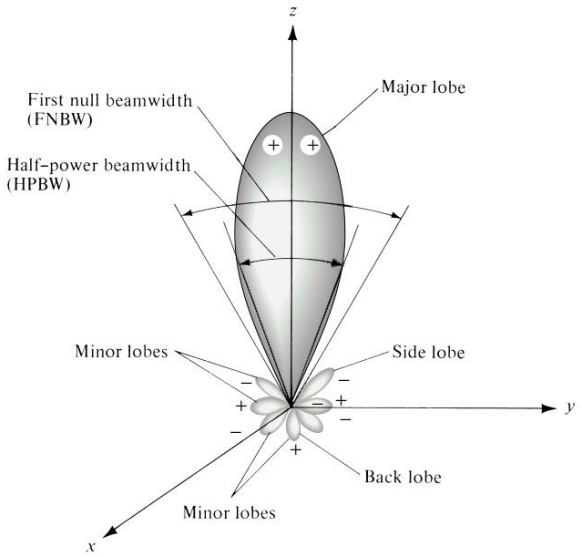

Figure 16. *The radiation pattern of an antenna with different lobes [16]*

Half Power Beam Width (HPBW)

The angle between points in the direction of the major lobe at which the magnitude of the radiated power includes the half power of the maximum value or decreases by 3 dB, is called the HPBW. Radians or degrees are used for its measurements. As can be seen in Figure 16, First Null Beam Width (FNBW) is another type of the beam width, which is referred to the measuring of the angle between the first nulls on the main lobe [16].

Input Impedance

The ratio of voltage to current at the input terminals of the antenna is called input impedance of the antenna. The antenna impedance is a complex parameter, as expressed in (4.14). The real part represents the amount of power that is radiated or absorbed within the antenna and contains two elements, radiation resistance and loss resistance. The imaginary part known as the reactance of the antenna, demonstrates the energy, which is stored in the near field of the antenna. Figure 17 shows the Thevenin equivalent circuit of an antenna in transmitting mode with a source. The impedance of the connected source is defined in equation (4.15) [16].

$$Z_A = R_A + jX_A = (R_r + R_L) + jX_A \tag{4.14}$$

$$Z_g = R_g + jX_g \tag{4.15}$$

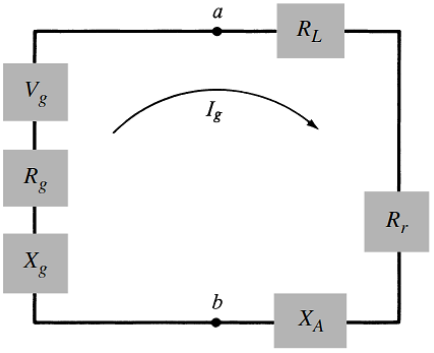

Figure 17. *Thevenin equivalent circuit of an antenna with a source in transmitting mode [16]*

The generated power by source consists of radiation power of the antenna, dissipated power of the antenna and dissipated power at the internal resistance of the generator. To have full transmission and deliver the maximum power to the antenna, the impedance of the antenna should be conjugate matched source as follow [16],

$$R_g = R_r + R_L \tag{4.16}$$

$$X_A = -X_g \tag{4.17}$$

In this state, half of power from source is dissipated at its internal resistance as heat and the delivered energy to the antenna is only the other half of the power. If the antenna can

achieve the 100% of the efficiency, then the total power delivered to the antenna can be radiated [16].

In the receiving mode, when the antenna acts as a receiver and it contains conjugate matching, half of the total power, which is collected by the antenna, is delivered to the load and the other half is scattered and dissipated as heat by the antenna. Figure 18 shows the Thevenin equivalent circuit of the antenna in the receiving mode. Since the input impedance of the antenna depends on the frequency; the antenna will be conjugate-matched only within a certain frequency bandwidth. In addition, the antenna impedance is dependent upon many other factors containing the antenna geometry, the used method for its excitation and the vicinity of objects in its surrounding. Due to complex geometries of the antennas, their input impedance is usually determined experimentally instead of analytically [16].

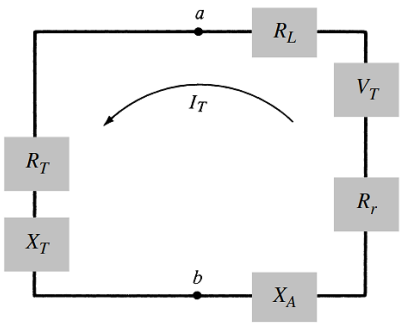

Figure 18. *Thevenin equivalent circuit of an antenna with a source in receiving mode [16]*

Directivity and Gain

The directivity of an antenna measures the radiation power in a given direction as compared to averaged radiation intensity in all directions. Therefore, it can be defined as the ratio of the maximum power P_{max} (W/m^2) to the average power P_{ave} (W/m^2) of the antenna using the (4.18) [16],

$$D = \frac{P_{max}}{P_{ave}} \tag{4.18}$$

Antenna gain has a close definition to antenna directivity, while the effect of the antenna radiation efficiency is considered to calculate it as follow [16],

$$G = kD \tag{4.19}$$

where k is the efficiency of the antenna and can be obtained by [16],

$$k = \frac{P_{rad}}{P_{in}} = \frac{P_{rad}}{P_{rad} + P_{loss}} \tag{4.20}$$

where P_{rad} is the radiated power of the antenna and P_{loss} is the power dissipation.

As a result, antenna gain measures how much power is transmitted in the direction of the maximum radiation as compared to the ideal antenna called Isotropic Antenna. The isotropic antenna radiates power equally in all directions. Although there is no physical antenna in reality, it is used as a reference antenna to achieve the gain of antenna [16].

Antenna Gain is sometimes described as a function of the arrival angle. In this case, it is necessary to plot the radiation pattern, which demonstrates the variation of the power radiated by an antenna in the antenna's far field. The gain of antenna is referred to the dBi unit. The dBi unit represents the decibels relative to an isotropic antenna [16].

Antenna Efficiency

Determining how much energy is dissipated during the power is radiated and captured by the antenna is known as the antenna efficiency. The mismatching between the transmission line and antenna, the ohmic and heat loss related to the antenna structure and/ or the lossy materials close to the antenna. The total efficiency can be obtained by [16],

$$e_o = e_r e_{rad} \tag{4.21}$$

where e_r is the reflection (mismatch) efficiency and e_{rad} is the radiation efficiency. Radiation efficiency (e_{rad}) contains the radiation loss and ohmic losses within the antenna, can be calculated by,

$$e_{rad} = \frac{R_{rad}}{R_{rad} + R_{ohmic}} \tag{4.22}$$

Reflection efficiency (e_r) is used to measure the power loss, which occurs when the transmission line and antenna are not matched properly. Thus, e_r is defined as,

$$e_r = 1 - |\Gamma|^2 \tag{4.23}$$

where Γ denotes the reflection coefficient [16].

Polarization

Polarization of the antenna evaluates the polarization of the electromagnetic wave in the far field produced by the antenna. The designed antenna can be categorized based on the polarization of a wave radiated into linearly polarized, circularly polarized and elliptically polarized antenna. Polarization mismatch explains that the receiving and transmitting antennas act with different types of polarization, which results in losing a certain amount of power from the applied signal. In order to determine the amount of power loss due to mismatching of the polarization, the polarization loss factor (PLF) is defined as,

$$PLF = |\overline{\rho_r} \cdot \bar{\rho}_t|^2 = cos^2\psi_p \tag{4.24}$$

where ρr is the polarization vector of the receiving antenna, ρt denotes the polarization vector of the transmitting antenna and ψ_p shows the angle difference. If both antenna

include the same polarization the PLF will be unity, which means that the maximum power from the transmitting antenna can be captured by receiving antenna [16].

Friis Transmission Equation

The Friis transmission equation is one of the most fundamental equations in antenna theory, which provides the relationship between the power received by one antenna and the power transmitted from another antenna separated by a determinate distance. The general form of this equation is written as [16],

$$\frac{P_r}{P_t} = e_{rt} D_t e_{rr} D_r (1 - |\Gamma_t^*|^2)(1 - |\Gamma_r^*|^2) \left(\frac{\lambda}{4\pi R}\right)^2 \text{PLF} \tag{4.25}$$

where R is the distance between the two antennas and the subscripts r and t denote the receiving and transmitting antennas, respectively. The term $(\lambda/4\pi R)^2$ is known as the free space loss factor, which measures the losses result from the spherical spreading of the electromagnetic wave. The receiving and transmitting antennas should be separated by a sufficiently large distance to satisfy [16],

$$R > \frac{2D^2}{\lambda} \quad (R \gg D \; and \; R \gg \lambda) \tag{4.26}$$

where D is the largest dimension of the antenna.

Friis equation can be used to study RF communication links, particularly in calculating link budget when designing antenna of RFID systems. The following assumptions are made for simplicity of the Friis equation: the reflection coefficient is equal to zero and two antennas have the same polarization. Hence, the simple form of Friis equation can be written as,

$$\frac{P_r}{P_t} = \left(\frac{c}{4\pi f R}\right)^2 G_t G_r \tag{4.27}$$

According to the above equation, the received power and frequency have inverse relationship, which means that the higher operating frequencies increase the energy loss of receiving antennas [16].

Radar Range Equation and Radar Cross Section

The radar range equation (RRE) is used as one application of Friis transmission equation, which gives the proportion of the transmitted power of one antenna to the received power after it has been scattered by a target of radar cross-section σ. The complete radar range equation including impedance mismatch losses as well as polarization losses is written as [16],

$$\frac{P_r}{P_t} = \frac{e_{rt} D_t e_{rr} D_r}{4\pi} (1 - |\Gamma_t|^2)(1 - |\Gamma_r|^2)\sigma \left(\frac{\lambda}{4\pi R_1 R_2}\right)^2 \text{PLF} \tag{4.28}$$

where R_1 and R_2 represent the distances between the transmitting and receiving antenna with the target, respectively. The radar cross section (RCS) of a target σ is defined as the ratio of forward power density to the reverse power density of the electromagnetic wave scattered by the target. As the power is distributed in the shape of a sphere, the radar cross section is measured in,

$$\sigma = \lim_{R \to \infty} \left[4\pi R^2 \frac{W_s}{W_i} \right] \tag{4.29}$$

where W_i represents the scattered power density, W_s is the forward power density in the range, and R denotes the distance from the target [16].

4.3 RFID system

Radio Frequency Identification (RFID) is a wireless technology, which uses the electromagnetic fields in the radio frequency (RF) range, to identify physical objects. In RFID system, the reader as interrogators communicates wirelessly with the tags as transponder through the antenna to enable identification. The type of frequency, power source, and protocol selected in the RFID systems have significant effects on the range, cost, and features available to the user. Therefore, RFID systems are categorized based on the frequency of the radio waves used for them, the type of power source used for tags, and the protocols used to communicate between tag and reader [18].

Frequency Bands for RFID

RFID systems possess various characteristics due to operating in different range of frequencies, from around 100 kHz to over 5 GHz. It means that each frequency band contains the different optimal applications. The frequency of the radio waves used in RFID systems has important impacts on the read range, data rate and the behavior of RFID tags [18].

In brief, RFID systems can be classified into four categories in accordance with the operating frequencies as listed in Table 2. Also, the different types of tag antennas associated with various operating frequencies used in RFID systems are shown in Figure 19 [18].

- Low Frequency (LF) consists of 125–134 kHz of operating frequency that the transmission ranges are limited to centimeters or inches. The LF tags and readers are used for short-range applications like vehicle and animal identification.
- High Frequency (HF) consists of 13.56 MHz of operating frequency and the maximum read range is about 1 meter. HF systems have worldwide frequencies, which

are available to smart cards and labels such as RFID-equipped passports and travel documents.

- Ultra High Frequency (UHF) consists of 433, and 860-960 MHz of operating frequency that has much better read ranges (up to 10 meters). UHF readers are able to transfer data faster with active low power tags like using in supply chain management, transport baggage tracking, and asset tracking.
- Super High Frequency (SHF) consists of 2.4-2.45 GHz of operating frequency, known as microwave readers, has the highest read ranges up to 30 meters. Microwave readers are used in long-range tracking and fast data rates with active tags such as automatic vehicle identification.

Table 2. *The operating frequency of RFID systems [18]*

Definition	Frequency Band	Operation range (m)	Applications
Low Frequency (LF)	125-143 KHz	Up to 0.5	Vehicle and animal identification
High Frequency (HF)	13.56 MHz	Up to 1	Smart cards and labels
Ultra High Frequency (UHF)	433 MHz 860-960 MHz	Up to 10	Supply chain management and asset tracking
Microwave	2.4-2.45 GHz	Up to 30	Long-range tracking with active tags

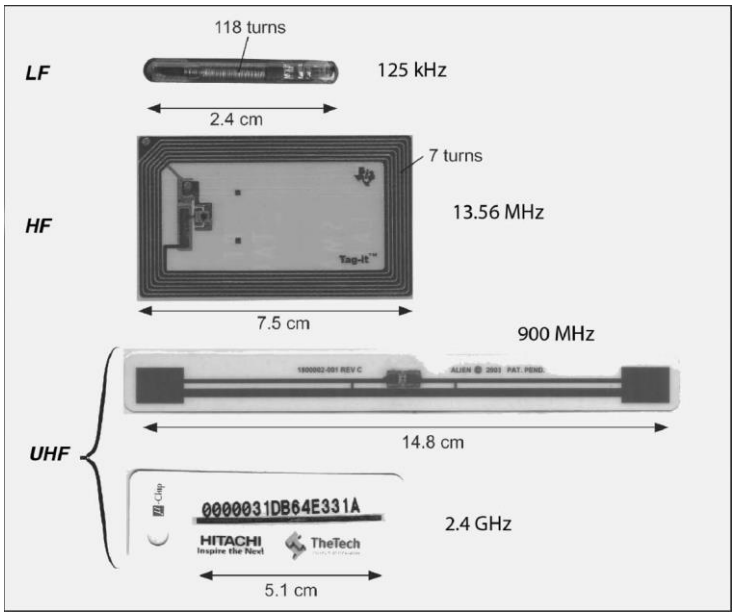

Figure 19. *Examples of tag antenna configuration designed for different operating frequencies [18]*

Passive, Semi passive, and Active Tags

The type of means, which used to provide power to the tags, can bring tremendous advantageous to RFID systems. For instance, the elimination of radio transmitter and battery from an RFID tag can reduce the cost and size of the RFID systems. RFID systems have

been also categorized into passive, semi-passive and active based on the presence or absence of these components as the power source of the tags as shown in Figure 20 [18].

Passive tags have no batteries to drive tags and no radio transmitter of their own. Passive tags do not need any power source but energize the tag using the electromagnetic waves from the reader and then their data are transmitted back (backscatter). In contrast, the semi-passive tag uses a local battery as a source of electrical power incorporate with the passive backscattering that allows the device to perform an operation. Active tags provide energy from both a local power source and a conventional transmitter and establish direct communication with the reader rather than using backscattered communications [18].

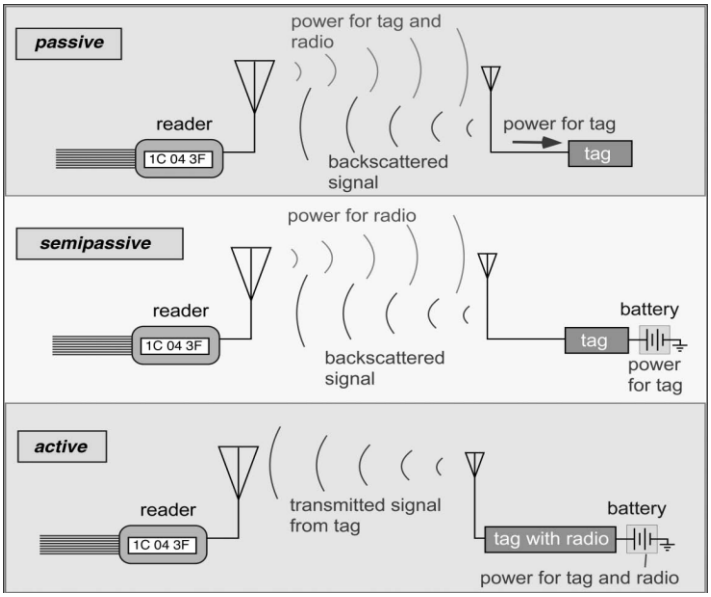

Figure 20. *Options for tag power source [18]*

4.3.1 RFID System Composition

The passive RFID tags are ubiquitous in many branches of modern engineering, with areas of applications including access control, file tracking, race timing, supply chain management, smart labels, etc. Moreover, due to the lower price of this tag configuration, it is used as more economical tags for industries. Passive RFID systems consist of a simple structure including a tag, a reader, antennas and a host computer as shown in Figure 21. In passive RFID systems, each individual object is labeled with a tag, which carries data for identification. The RFID tags consist of an integrated antenna with one integrated circuit (IC) which includes the tag ID and the logic that is required for navigating the protocol, which is used to guide discussions between the tag and reader. In addition, there is another antenna installed at the reader, which is a radio transmitter-receiver that sends a signal to a tag and read its response. Indeed, the antenna placed in the reader; transmit a signal using the radio frequency waves. Hence, the RFID tag gets into the electromagnetic field and the integrated antenna of the tag harvest energy from the reader. At the

receiving side, the RFID tag first rectifies and filters the appeared high frequency signal to the DC voltage and pump it to a required level to activate the IC. Then the information stored inside the tag is added to the RF signal and backscattered to the reader. Moreover, the reader is connected to a host computer as a user interface, which controls the reader for the establishment of the communication with tag and stores, and displays the resulting data from the tag [18].

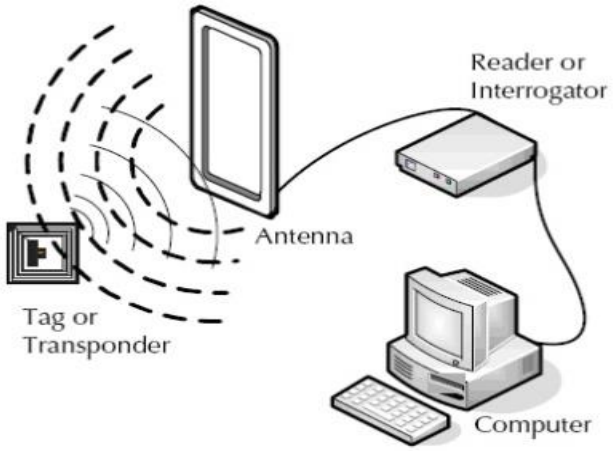

Figure 21. *RFID system composition*

The radio link between the reader and the tag is a duplex transmission, including the down-link transmission from the reader to the tag and the up-link transmission from the tag to the reader. These two links consist of encoding, decoding, modulation, and demodulation of the signal. In passive RFID system, the down-link signal is responsible for providing continuous energy for the RFID tag in addition to carrying data between the tag and reader. For this purpose, pulse-interval encoding (PIE) approach can be used where the binary '1' and '0' are respectively encoded and each binary is transmitted. In fact, after modulation, the level of signal will not always be zero during the interval of one symbol, which ensures the tag to achieve energy from the reader continuously. On the other hand, in the up-link, which known as the backscattered radio link in RFID system, the tag antenna is connected to loads with different impedances for various binaries. In this transmission, by changing the current on the tag antenna, the reflected electromagnetic field strength will change as well. As a result, the induced current on the reader antenna can be used to detect the transmitted signal from the tag by the strength modifying of the electromagnetic field [18].

4.3.2 Link Budgets and Power Transfer

Link budget determines the minimum power that is required to transmit a signal through a wireless link for receiving the transmitted data successfully. There are two link budgets separately for RFID systems including the down-link transmission from the reader to the tag and the up-link transmission from the tag to the reader. In the up-link when the reader high sensitivity is usually 75-90 dB, the power of backscattered is in the required range

for receiving successfully since the tag IC is energized [29]. In the down-link, the received power by tag is often around 10-30 μW to turn on the IC and read the information, also, it needs much more power around 30-100 μW for writing the new data. Thus, in down-link budget, the Friis transmission equation can be used to find the relationship between the tags received power and the reader transmitted power as follow,

$$P_{rx\_tag} = P_{tx\_reader} G_{tx\_reader} G_{rx\_tag} \left(1 - \left|\Gamma_{rx\_tag}{}^{*}\right|^2\right) \left(\frac{\lambda}{4\pi R}\right)^2 \tag{4.30}$$

where R is the distance between the reader and the tag. $\Gamma_{rx_tag}{}^{*}$is the power reflection coefficient because of the mismatching of the tag antenna and IC. In the interests of simplicity, we consider the IC as a linear load and antenna with open-circuit voltage and complex source impedance connected to IC as shown in Figure 22. The current of this circuit is obtained by,

$$I = \frac{V_{OC}}{(R_a + jX_a) + (R_{IC} + jX_{IC})} \tag{4.31}$$

The power transferred to the IC in this circuit can be expressed by,

$$P_{IC} = \frac{|I|^2 R_{IC}}{2} = \frac{{V_{OC}}^2 R_{IC}}{2\big((R_a + jX_a) + (R_{IC} + jX_{IC})\big)} \tag{4.32}$$

Besides, it is assumed that the reader antenna is conjugate matching to its source and the reader antenna and tag antenna are polarization matched. Therefore, $\Gamma_{rx\_tag}{}^{*}$ is equal to 0 and $R_a+jX_a= R_{IC}-jX_{IC}$. Finally, the maximum power transferred to the IC is calculated when the conjugate matched condition exists as,

$$P_{max} = \frac{V_{OC}^2}{8R_{IC}} \tag{4.33}$$

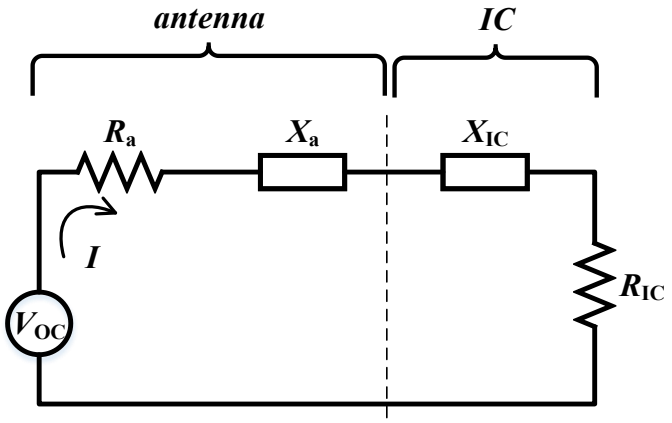

Figure 22. *Linear approximation of antenna and IC*

The power transfer coefficient (τ) defines as the ratio of the delivered power to the IC to the maximum power in equation (4.34). If the antenna is conjugate-matched to the IC, then the power transfer coefficient is the maximum value [18],

$$\tau = \frac{P_{IC}}{P_{max}} = \frac{4R_{IC}R_a}{|Z_{IC} + Z_a|^2} \tag{4.34}$$

when $\tau = 1$ means that the maximum power is transferred to the tag IC, and thus the tag read range is the maximum [18]. Also, the received energy by the tag IC can be expressed as [18],

$$P_{rx-IC} = \tau P_M \tag{4.35}$$

4.3.3 Impedance Matching and Tag Read Range

In RFID tags, different types of matching circuits and different ICs can be used depending on their applications. However, as shown in Figure 23 (a), the IC is usually assumed as approximated linear but complex load impedance connected to the antenna, which is electrically modeled as a voltage source [18]. The electrical model demonstrates in Figure 23 (b). There are three main parameters, antenna impedance, IC impedance, and read range that describe the performance of the tag antenna.

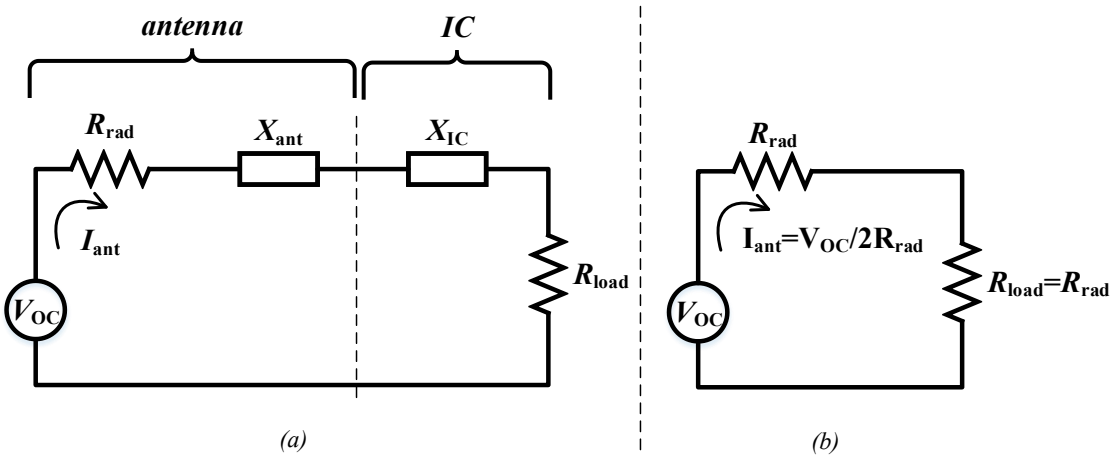

Figure 23. *(a) Linear approximation of antenna and IC (b) Conjugate-matched Case [18]*

As above-mentioned, the input impedance of the antenna should be conjugate-matched to the impedance of the load for achieving the maximum antenna radiation efficiency. Thus, the impedance matching of the RFID tag antenna is more crucial due to its effect on the power transferred to the IC. To energize the tag IC, it needs to receive power more than the threshold. The value of threshold can be applied to determine the maximum read range of tag by replacing the $P_{rx\text{-}tag}$ with P_{th}/τ, as derived in equation (4.36).

In fact, read range is the maximum distance of tags at which the information stored in the IC tag can be used by the reader. According to the equation (4.30), tag-received energy is inversely proportional to the distance between the tag and the reader, which means that if the distance between the tag and the reader is longer than the read range, the tag is hidden. The maximum tag read range can be calculated using the threshold value of the received power as follows,

$$R = \frac{\lambda}{4\pi}\sqrt{\frac{P_{tx\_reader}G_{tx\_reader}G_{rx\_tag}\tau}{P_{th}}} \tag{4.36}$$

where P_{th} is the equivalent transmitted threshold power. According to the above equation, the read range is proportional to the gain of the tag antenna and the power transfer efficiency that both quantities are dependent on frequency.

As can be seen in Figure 24, the tag resonance frequency is defined as the frequency where the read range reaches to its peak value, while the impedance has the highest value in different frequency referred as the tag antenna self-resonance frequency [29].

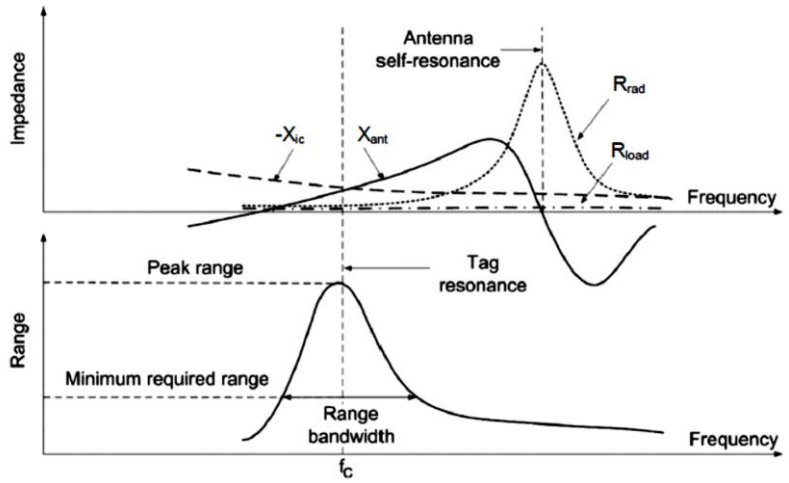

Figure 24. *Antenna impedance, IC impedance, and read range as functions of operation frequency [29]*

Moreover, it can be also noted from the equation (4.36), the read range is proportional directly to the transmitted power; however, the transmitted power has regulatory limitations. Therefore, this regulatory limitation for the transmitted power is defined by communications regulation organizations in different countries. For example, in European countries, the transmitted power must not exceed 3.28 W (EIRP=3.28 W). These regulatory limitations are defined as effective isotropic radiated power (EIRP) values, which is a function of received and transmitted power of an antenna and calculates the peak power density of the transmitted signal written as,

$$\text{EIRP}=P_{tx}(dBm) + G_{tx}(dBi) \tag{4.37}$$

5. DESIGN, IMPLEMENTATION AND MEASUREMENTS

5.1 Over View of the Designed System

The designed RF energy harvesting system integrates two main units; an energy harvesting unit and an RF switch unit. Figure 25 depicts the designing steps of the energy harvesting system. Our aim of this study is to harvest the receiving RF signal and convert it to the DC voltage and charging a storage capacitor. When the voltage at the capacitor exceeds to the threshold voltage of the PIN diode, the pin diode will turn ON and dipole antenna used in the RF switch unit is connected to RFID IC. Therefore, RFID reader starts getting the response from the RFID IC. This system is designed and optimized for the European UHF RFID spectrum from 865.7 MHz to 867.7 MHz, which is suitable for wireless power transmitting continuously and power on a passive UHF RFID tag. The designed procedures of each unit and its simulation results are explained in the following sections and the measurement results of the fabricated prototype are presented.

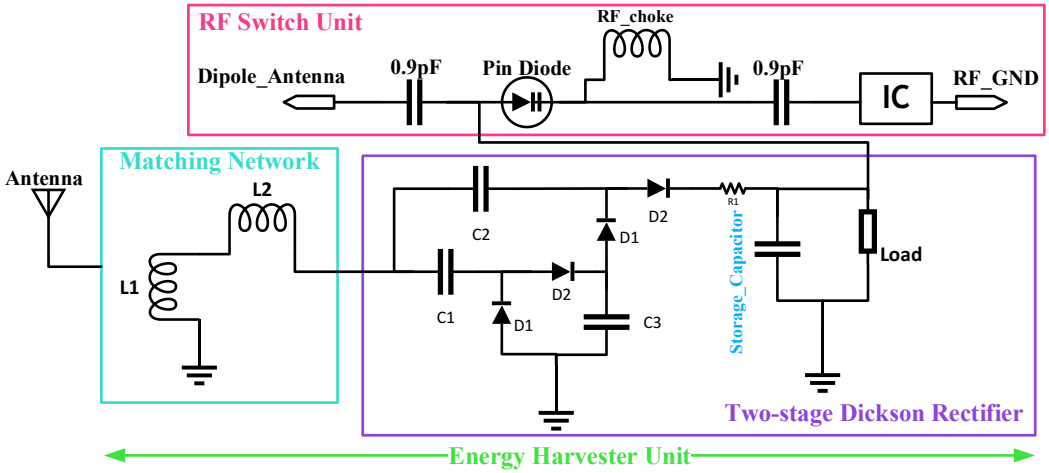

Figure 25. *The block diagram of the designed RF energy harvesting system integrating an RF switch*

5.2 Design Procedure and Simulation Results

Energy Harvesting Unit

The energy harvesting unit consists of a receiving antenna, an L-matching impedance network, a two-stage Dickson rectifier, and a storage capacitor. In this work, an RF signal generator is used as an RF power source at the frequency of 866 MHz, which generates a continuous-wave (CW) and accurate input signal for conversion.

The most crucial part of designing the energy harvesting unit is related to the impedance matching network and the rectifier. For this purpose, first, a circuit with two voltage doubling stages, known as a two-stage Dickson charge pump, was designed to rectify the RF input power to DC voltage. We considered two stages of voltage doubler to ensure the sufficient DC output voltage to turn ON the PIN diode placed in the RF switch unit. Since Schottky diodes have the lowest possible threshold voltage and operate as very fast switches at high frequencies, the zero-bias Schottky detector diodes Avago's HSMS-286K with two capacitors, as shown in Figure 25, were employed in each stage. Each SOT-363 package of HSMS-286K contains two diodes, hence, two package was enough for fabricating the circuit and save the circuit size. Furthermore, 56 kΩ was chosen as the load. To determine the time constant, a 56 Ω was used in series with the 11 mF capacitor, which employed as the energy storage. The storage capacitor that is used in this study, is a thinnest and smallest chip type of the electric layer capacitor (EDLC), which can charge up to 3.3 V [30].

The SPICE parameters of the Schottky diodes are provided by Agilent in the data sheet, which are listed in Table 3. These parameters were applied to the Advance Design System (ADS) simulator to model the diodes by its equivalent circuit [31].

Table 3. *The SPICE parameters of the Schottky diodes [31]*

Parameters	Units	Value
B_V	V	7.0
C_{J0}	pF	0.18
E_G	eV	0.69
I_{BV}	A	1 E-5
I_S	A	5 E-8
N		1.08
R_S	Ω	6.0
P_B(VJ)	V	0.65
P_T(XTI)		2
M		0.5

By neglecting the effect of the diode substrate, the linear circuit model of Schottky diode can be demonstrated as Figure 26.

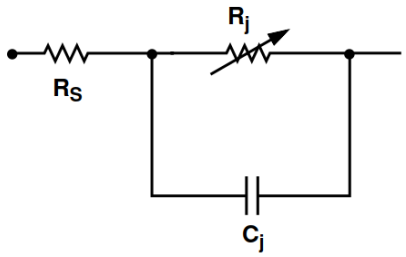

Figure 26. *Equivalent linear circuit model [31]*

where R_S is the series resistance, C_j shows the junction capacitance and R_j can be calculated by,

$$R_j = \frac{8.33 \times 10^{-5} nT}{I_b + I_s} \tag{5.1}$$

where I_b is the externally applied bias current in A, I_S is the saturation current, T denotes temperature in Kelvin and n shows the ideality factor [31].

By using the SPICE parameters, a simplified schematic of a two-stage Dickson charge pump was generated in the ADS simulator. Due to the non-linearity of Schottky diodes employed as the rectifying elements, the input impedance of the rectifier varies as a function of both frequency and incident power [2][31]. Thus, the Harmonic Balance (HB) was used for simulating the output voltage of the circuit versus the RF input power. In addition, Large-Signal S-parameter (LSSP) analysis method was utilized to measure the reflection coefficient of the circuit versus the frequency while sweeping the RF input power. LSSP analysis technique is a non-linear simulation that is used for the power level-dependent behavior of the diode [32].

On the other hand, designing a matching network stage plays a crucial role in tuning the impedance match properly between the RF source and the rectifier to reduce the transmission loss and enhance the output DC voltage. To achieve this, first, we kept the operating frequency fixed at 866 MHz and observed the changes of resulting on the output voltage value while sweeping the level of RF input power by using the HB simulation. Then, we determined the RF input power at which the output voltage value reached the voltage that was required for turning on the PIN diode in the RF switch unit. As we discussed later, the typical threshold voltage of the selected PIN diode is 0.85 V. Hence, the required RF input power level to achieve 0.85 V was about -13.5 dBm.

After that, we added two lumped elements as an L-matching network to tune the impedance matching. In this work, we used two inductors. Due to the parasitic characteristics of the RF components, it was required to add transmission lines between components. Hence, the width and length of the transmission lines were calculated by applying the FR4 substrate parameters in the ADS calculator. Next, we fixed the RF input power at the desired value and the input reflection coefficient of the circuit against sweeping the frequency was simulated using the LSSP analysis technique.

In order to provide the maximum power transmission at 866 MHz, we varied the value of the inductors from 1nH to 38nH with 0.2nH step size. As it is required to match the input impedance of the rectifier accurately to the output impedance of the RF source, we also optimized the length of the transmission lines and the capacitors values that were used in the charge pumps structure. The optimum value used for the width and length of the transmission lines were 2.96 mm and 3.75mm, respectively. Table 4 summarizes the components values used to design the energy harvesting unit.

Table 4. *The components value used in the energy harvesting unit*

Component	Value
L1	2.7 nH
L2	22 nH
C1	1.2 pF
C2	2.7 pF
C3	2.7 pF
Storage-capacitor	11 mF
R_1	56 Ω
Load	56 KΩ
Schottky diode	HSMS-286K

Figure 27 demonstrates the simulation of output DC voltage with and without impedance matching network. Finally, after designing this unit, the return loss at the desired frequency of 866 MHz, while sweeping the RF input power is shown in Figure 28.

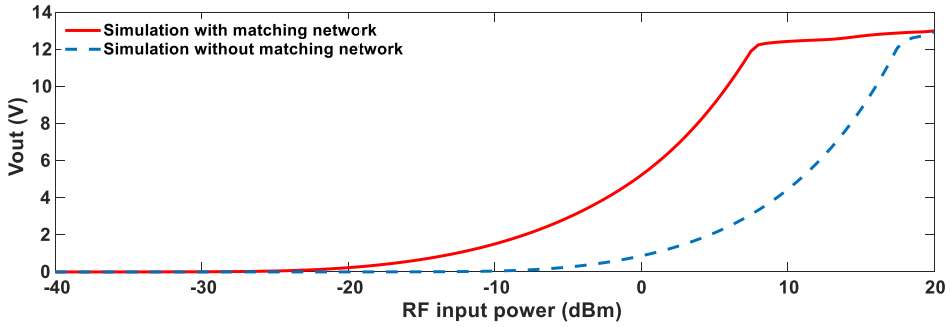

Figure 27. *The output DC voltage of the RF rectifier with and without impedance matching network*

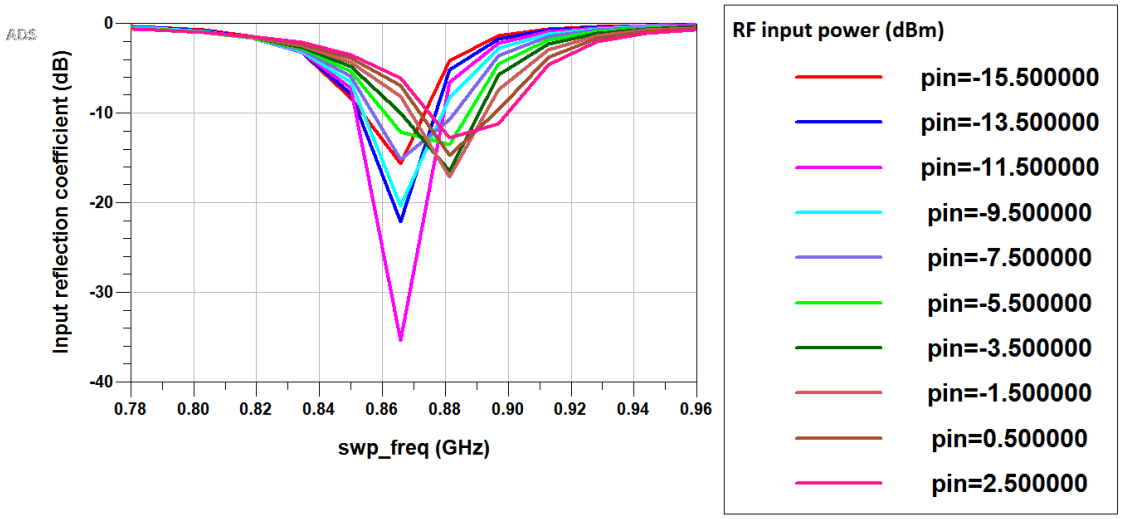

Figure 28. *The input reflection coefficient versus frequency with sweeping the input power*

RF Switch Circuitry

In the next step, the RF switch, which consists of a pin diode, RFID IC, DC blocking capacitors, an RF blocking choke, and a dipole antenna, was designed and simulated. The RF switch circuitry is responsible for activating the IC tag, as displayed in Figure 25. To this end, a series SPST switch structure was used to design the RF switch. Because this type of structure can be employed in the RF frequency range with the low insertion loss level.

We used the SMP1340-079LF of plastic packaged PIN diodes in this configuration. Due to possessing the short carrier lifetime of 100nS typically in combination with the thin "I" region of 5 µm, this model of PIN diode is a suitable component for fast switching speed with a low capacitance at RF frequencies. In addition, the low ON resistance of 0.85 Ω in this model of diode results in decreasing the insertion loss and power dissipation. The typical forward voltage of this PIN diode is 0.85V [33].

In this approach, when the storage capacitor starts charging and the output DC voltage of the rectifier reaches to the threshold voltage of the PIN diode (0.85 V), The Pin diode will be turned ON. Then, the ON forward resistance of the diode is exhibited between the output of rectifier and load and all incident power can be passed. Thus, the DC voltage can control the DC bias through the pin diode and RF choke. On the other hand, a dipole antenna, which was modelled in the ANSYS HFSS (full-wave electromagnetic field solver based on the finite element) V15 simulator, as explained later, provides the RF signal. Then the 0.9 pF capacitor is employed as a DC block. After that, the signal can take out through the IC by using a 0.9-pF series coupling capacitor. Consequently, the RFID IC can be read.

The dipole antenna, which is used in the RF switch unit, is a previously designed and fabricated prototype in [34]. This type of antenna is used widely for passive UHF RFID tags. Figure 29 shows the geometrical parameters of the dipole antenna [34].

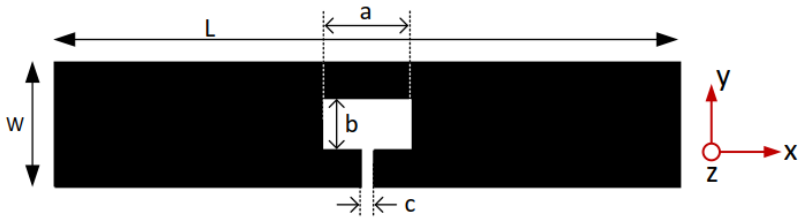

Geometrical parameters in millimeters.

L	W	a	b	c
100	20	14.3	8.125	2

Figure 29. *The geometrical parameters of the fabricated prototype dipole antenna [34]*

In order to use the dipole antenna, it was required to match the antenna impedance to the impedance of the circuit seen from the dipole antenna at the desired frequency. Therefore, it was required to be optimized. For this purpose, first, the impedance of circuit seen from the dipole antenna was simulated using the ADS simulator. To obtain this impedance, the input of energy harvesting unit was terminated by 50 Ω and the RF source was connected to the switch circuitry. The simulated impedance seen from antenna was Z=0.117-j211.742.

After that, the antenna was optimized to match the achieved impedance of the circuit without considering any ground traces. The optimization of the antenna was done by changing the geometrical parameters of the dipole antenna including the length (a) and width (b) of the slot using the ANSYS HFSS V15 simulator. Thus, geometrical parameters of the antenna were modified as listed in Table 5.

Table 5. *The optimized geometrical parameters of the dipole antenna*

Geometrical parameters	Value (mm)
L	100
W	20
a	14
b	9
c	2

In fact, the simulated read range of the optimized dipole antenna was about 15 meters, whereas, ground traces were not considered in the simulation and optimization of the dipole antenna. The value of simulated read range with the ground traces was about 1.13 meters. Hence, as a future work, the antenna should be optimized to improve the read range.

In the next step, the RF switch unit was connected to the energy harvesting unit and simulated the whole circuit. In order to do the simulation, the S-parameters model of the PIN diode provided by the Skyworks solution, Co. associated with the model of the optimized antenna extracted from HFSS were used. In addition, the tag IC, which was used in this work, was NXP UCOD G2iL series RFID IC. It was manufactured in a fixture patterned using copper on a plastic film. The equivalent circuit of the tag IC including a resistance of 2.85 kΩ in parallel with the capacitance of 0.91 pF was employed [34].

As studied in the simulation of the rectifier with matching network in Figure 29, the output voltage reaches to 0.85 V at the input power of about -13.5 dBm. Hence, we set the input power at -13.5 dBm and then the RF switch circuitry was added to the rectifier, the input impedance matching must be tuned again. Therefore, the L1 of 2.7 nH was replaced by 2.2nH. The output DC voltage of the whole system is demonstrated in Figure 30.

As it is clear in Figure 30, the level of the output DC voltage decreases compared to the output voltage of the system without the RF switch circuitry but still the required voltage

for power on the PIN diode can be provided at low power. Figure 31 shows the reflection coefficient of the whole system for different input power.

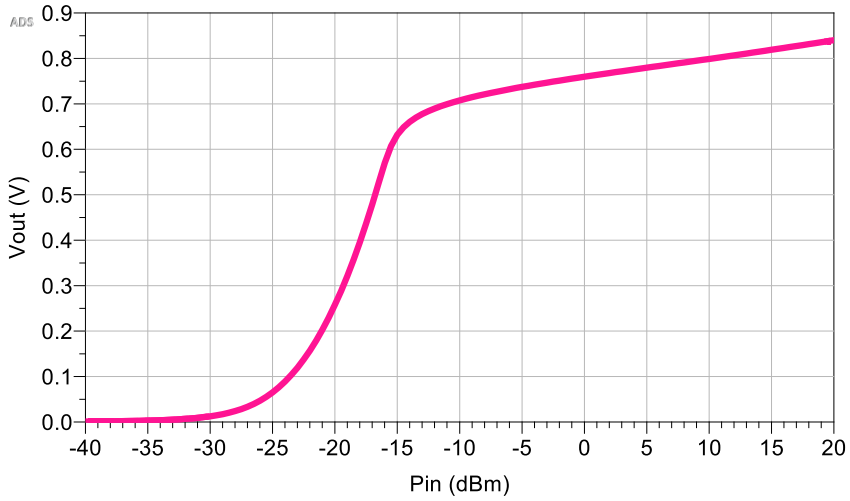

Figure 30. *The output DC voltage of the whole energy harvesting system*

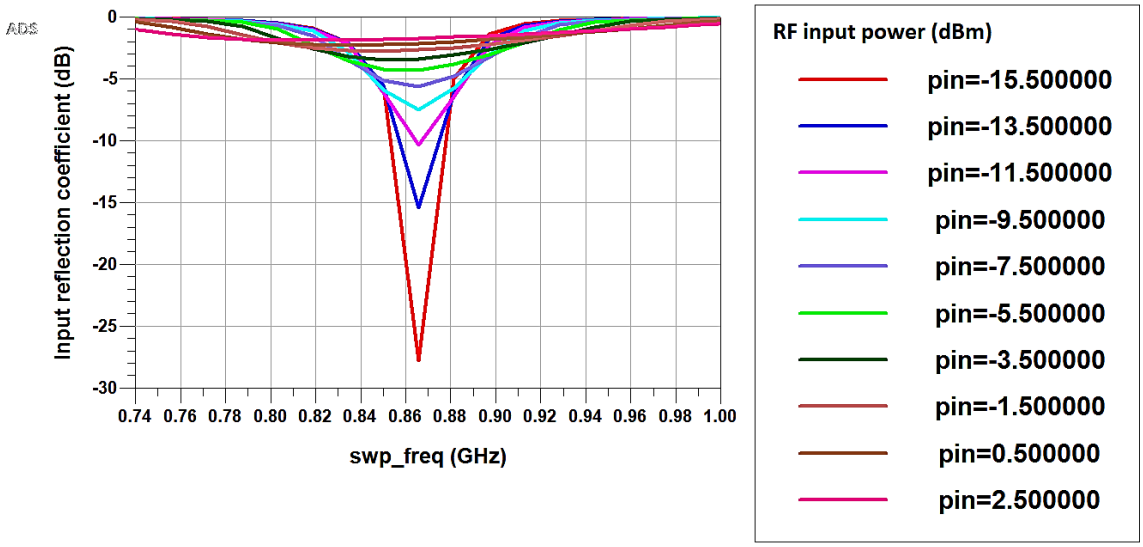

Figure 31. *The input reflection coefficient of the whole energy harvesting system*

As is obvious in Figure 31, the designed energy harvesting system works properly at the lower input power at the target frequency of the 866 MHz.

5.3 Fabrication and Measurement Results

We fabricated the designed RF energy harvesting system on FR4 substrate and connected it to a 50 Ω RF source via an SMA connector. In addition, we attached the 3×3 mm^2 pads of the tag IC fixture between the antenna and the capacitor of 0.9 pF placed in the RF switch with conductive epoxy. Figure 32 depicts the fabricated circuit board.

First, we measured the input reflection coefficient of the RF energy harvesting circuit through a Vector Network Analyzer (VNA). According to this measurement, the achieved components values of matching network in simulation, could not properly match the input impedance of RF rectifier to the output of the source. In reality, the peak value of the input reflection coefficient shifted frequency from 866 MHz and its magnitude is not sufficiently small. Hence, it should be tuned on the PCB.

To tune the matching network in practice, we varied the value of the inductors and observed the results that how the matching components affect the reflection coefficient. The series inductor in the matching network had an effect on the frequency shifting and the parallel inductor had an impact on the magnitude of the reflection coefficient. As a result, L=10 nH for the series inductor and L=5.6 nH for the parallel inductor were the optimum values, which could obtain for L-network matching at 866 MHz to transfer the maximum power to the rectifier. Although, these matching components values were completely different with the simulation results, the measured peak of the input reflection coefficient tuned at 866 MHz. Figure 33 shows the measured input reflection coefficient for different input power level.

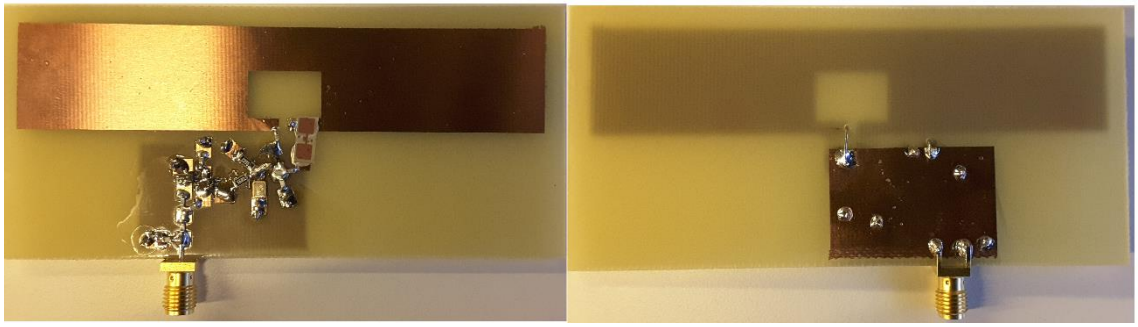

Figure 32. *The fabricated RF energy harvesting system*

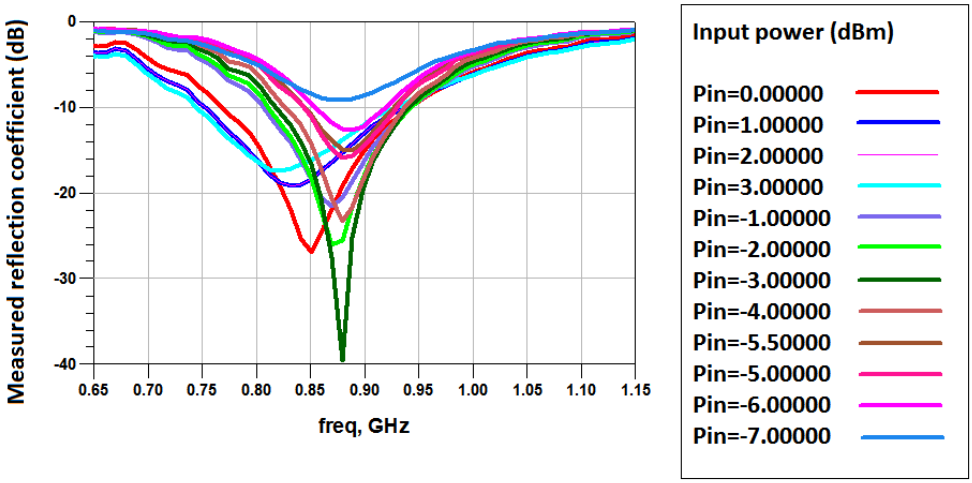

Figure 33. *The input reflection coefficient of the fabricated energy harvesting circuit*

After that, a generated continuous-wave (CW) by the RF signal generator at 866 MHz was fed into the rectifier. Afterward, the Voyantic Tagformance lite was used as a UHF RFID measurement system to analyse the tag behaviour. In addition, we connected the output of the RF rectifier to the Voltage Multimeter to follow the capacitor charging. Then, the fabricated board was located in the Voyantic anechoic chamber, which is coated by absorbers, hence, it avoids any reflections. Figure 34 demonstrates the measurement setup, where the circuit board was placed at the distance of 39.7 cm from the reader.

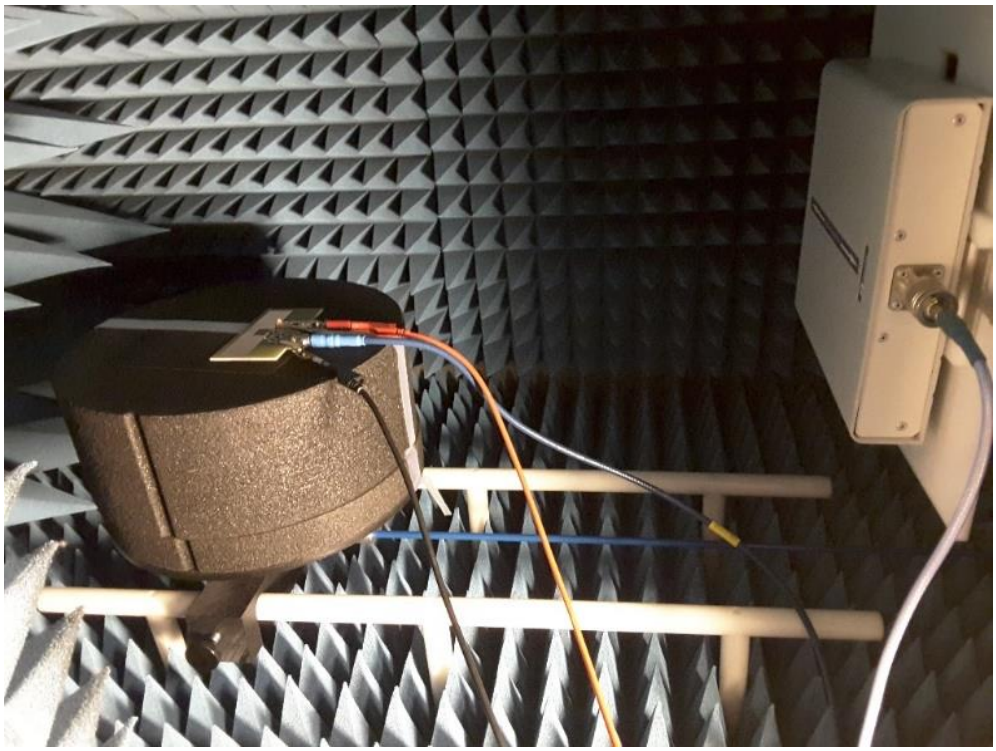

Figure 34. *The measurement setup of the fabricated energy harvesting system*

According to achieved reflection coefficient magnitude for various input powers, the output power of the generator, first, set at −7 dBm. Then, it varied by the step size of 0.5 dBm to observe at which power the IC tag has a response. By injecting less input power, for example, −7 dBm, the capacitor took about 5 minutes to charge up to 0.633 V for having any response of IC tag compared with the 1 minute and 30 seconds for −5.5 dBm of input power. Consequently, we set the RF signal generator with the −5.5 dBm as the optimum power to continue the measurements.

We did measurements in two phases and in each phase; we checked the IC response when the RF switch was turned ON or OFF. At the charging phase, whenever, the signal generator is not fed to energy harvester, the IC does not have any response. When the CW is injected to the rectifier, it converts the RF to DC signal and charges the 11mF capacitor. As soon as, the output of the capacitor approaches 0.633 V, the PIN diode is turned ON and the IC is read.

At the discharging phase, once the signal generator is not applied to the input, the storage capacitor starts discharging quickly through the load and, hence, reading is stopped at the 0.56 V. Figure 35 illustrates the performance of the designed RF energy harvesting system.

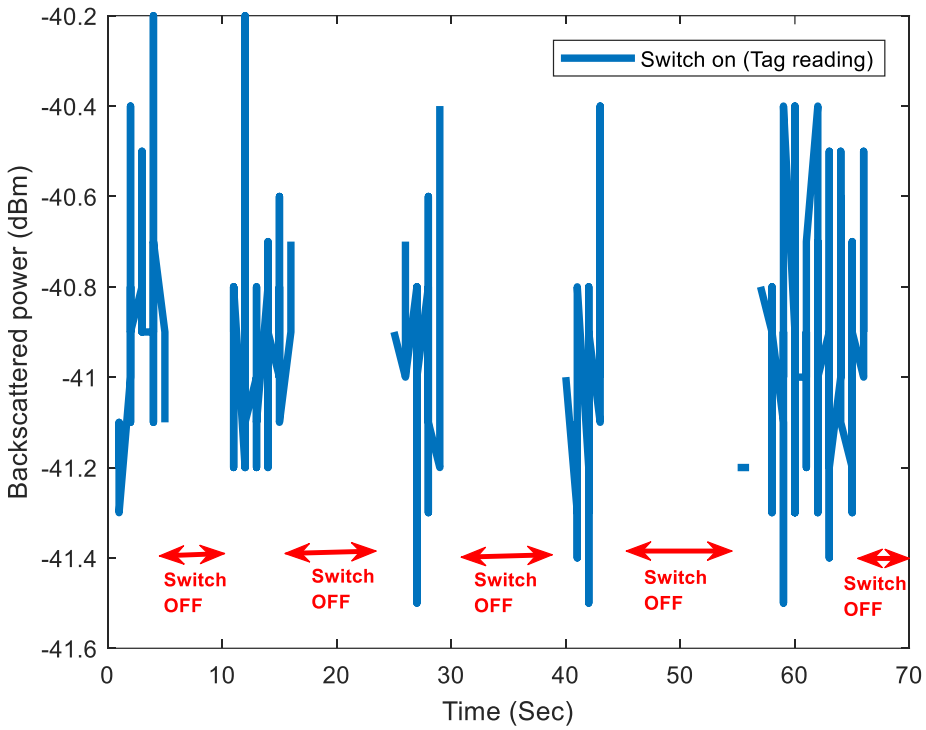

Figure 35. *The performance of the designed RF energy harvesting system*

6. CONCLUSIONS

In this master thesis, the design, simulation, and fabrication of the RF energy harvesting system are studied. As the first attempt, a two-stage Dickson charge pump based on Sckottky diodes is simulated. By using the Dickson topology and the characteristics of the diode, input RF signal is converted to DC voltage. The output DC voltage level is dependent on various parameters such as the number of stages, load value, capacitors, and the most significant impedance matching. Therefore, the effects of all these parameters are considered during designing and applied to the simulation. In this work, two RF inductors are used in an L-network matching circuit. Additionally, the output DC voltage is simulated before and after adding the matching circuit. The other important part of this project is related to the RF switch, which is responsible for power on the RFID tag. Hence, it is configured by the SPST switch structure and used a dipole antenna to provide the RF signal. This system was fabricated on the FR4 board as the substrate and connected it to a 50 Ω RF source via an SMA connector. After fabrication the system, the input impedance matching circuit is needed to tune more accurately to transmit the maximum available power to the RF rectifier. The input power level variation has effect on the input impedance of rectifier. Therefore, the circuit should be matched in all range of RF input power. According to the measurement results; the circuit is perfectly matched at the desired UHF frequency range with a sufficient power to wake-up the RFID IC. For−5.5dBm input power at 866 MHz, 0.633 V is obtained across the 56 KΩ at the output of rectifier to charge up the storage capacitor, turn on the RF switch and finally activates the RFID tag to get a response.

Moreover, a fabricated prototyped antenna was used in this project, which was essential to match its impedance to the circuit. To this end, the geometrical parameters of the antenna was modified. The RFID IC has a response at the target frequency with the proper power but in the cost of the read range, which is happened due to the ground traces using in the circuit board.

Although the performance of the energy harvesting system is verified in both the simulation and measurement, the designed circuit in the project still requires improvement to increase the read range by declining the effects of the ground traces and optimizing the dipole antenna. In addition, in the future, the configuration of the RF switch will be studied further to achieve a system where a single antenna is used for both energy harvesting RFID operation.

7. PUBLICATIONS

I. Nikta Pournoori, M. Waqas. A. Khan, Leena Ukkonen, Toni Björninen, "RF Energy Harvesting System Integrating a Passive UHF RFID Tag as a Charge Storage Indicator," submitted in *IEEE International Symposium on Antennas and Propagation,* Boston, Massachusetts, USA, July 2018.

REFERENCES

[1] Lu X, Wang P, Niyato D, Kim DI, Han Z. Wireless networks with RF energy harvesting: A contemporary survey. IEEE Communications Surveys & Tutorials. 2015 May; 17(2):757-89.

[2] Hameed Z, Moez K. Design of impedance matching circuits for RF energy harvesting systems. Microelectronics Journal. 2017 Apr 30; 62:49-56.

[3] Dai H, Lu Y, Law MK, Sin SW, Seng-Pan U, Martins RP. A review and design of the on-chip rectifiers for RF energy harvesting. InWireless Symposium (IWS), 2015 IEEE International 2015 Mar 30 (pp. 1-4). IEEE.

[4] Nimo A, Gric D, Reindl L.M. Optimization of passive low power wireless electromagnetic energy harvesters. Sensors. 2012; 12(10): pp. 13636-13663.

[5] Energy Harvesting Forum, Energy Harvesting Electronic Solutions for Wireless Sensor Networks and Control Systems [Online]. Available from: http://energyharvesting.net/

[6] Hameed Z, Moez K. Hybrid forward and backward threshold-compensated RF-DC power converter for RF energy harvesting. IEEE Journal on Emerging and Selected Topics in Circuits and Systems. 2014 Sep;4(3):335-43.

[7] Kim S, Vyas R, Bito J, Niotaki K, Collado A, Georgiadis A, Tentzeris MM. Ambient RF energy-harvesting technologies for self-sustainable standalone wireless sensor platforms. Proceedings of the IEEE. 2014 Nov;102(11):1649-66.

[8] Gudan K, Shao S, Hull JJ, Ensworth J, Reynolds MS. Ultra-low power 2.4 GHz RF energy harvesting and storage system with− 25dBm sensitivity. InRFID (RFID), 2015 IEEE International Conference on 2015 Apr 15 (pp. 40-46). IEEE.

[9] Nintanavongsa P, Muncuk U, Lewis DR, Chowdhury KR. Design optimization and implementation for RF energy harvesting circuits. IEEE Journal on emerging and selected topics in circuits and systems. 2012 Mar;2(1):24-33.

[10] Hong SS, Ibrahim RB, Khir MH, Zakariya MA, Daud H. WI-FI energy harvester for low power RFID application. Progress In Electromagnetics Research C. 2013;40:69-81.

[11] Aparicio MP, Bakkali A, Pelegri-Sebastia J, Sogorb T, Llario V, Bou A. Radio frequency energy harvesting-sources and techniques. InRenewable Energy-Utilisation and System Integration 2016. InTech.

[12] Valenta CR, Durgin GD. Harvesting wireless power: Survey of energy-harvester conversion efficiency in far-field, wireless power transfer systems. IEEE Microwave Magazine. 2014 Jun;15(4):108-20.

[13] Kuhn V, Lahuec C, Seguin F, Person C. A multi-band stacked RF energy harvester with RF-to-DC efficiency up to 84%. IEEE Transactions on Microwave Theory and Techniques. 2015 May;63(5):1768-78.

[14] Keyrouz S. Practical rectennas: far-field RF power harvesting and transport.

[15] Pozar, D.M. Microwave Engineering. The USA, Addison-Wesley Publishing Company. 1990. 719 p.

[16] Balanis, C.A. Antenna Theory Analysis and Design. 2nd ed. The USA, John Wiley & Sons, Inc. 1997. 931 p.

[17] Wong YC, Tan PC, Ibrahim MM, Syafeeza AR, Hamid NA. Dickson Charge Pump Rectifier using Ultra-Low Power (ULP) Diode for BAN Applications. Journal of Telecommunication, Electronic and Computer Engineering (JTEC). 2016 Dec 1;8(9):77-82.

[18] Dobkin DM. RF in RFID: Passive UHF RFID in Practice. Elsevier; 2008.

[19] Schneuwly A, Gallay R. Properties and applications of supercapacitors: From the state-of-the-art to future trends. Rossens, Switzerland. 2000 Oct.

[20] International Electrotechnical Commission, Electrical Energy Storage [Online]. Available from: http://www.iec.ch/whitepaper/pdf/iecWP-energystorage-LR-en.pdf

[21] Doherty WE, Joos RD. The pin diode circuit designers' handbook. Microsemi Corporation. 1998;1.

[22] Agilent Technologies, Datasheet: Understanding RF/Microwave Solid State Switches and their Applications; 2010 May 21. Available from: http://home.sogang.ac.kr/sites/eemic/lecture/note02/Lists/b26/Attachments/2/RF-switches.pdf

[23] Skyworks, Datasheet: Design with PIN Diodes; 2012 Oct 22. Available from: http://www.skyworksinc.com/uploads/documents/Design_With_PIN_Diodes_200312D.pdf

[24] Palomera-Arias R. PIN diode switch circuit for short time high current pulse signal (Doctoral dissertation, Massachusetts Institute of Technology).

[25] Cory R, Solutions S. RF/Microwave Solid State Switches. MPD/Microwave Product Digest (May 2009). Google Scholar. 2009 May.

[26] Stutzman, W.L. Thiele, G.A. Antenna Theory and Design. 2nd Edition. The USA, John Wiley & Sons, Inc. 1998. 643 p.

[27] Sadiku MNO. Elements of electromagnetics. 2nd ed. Oxford University Press, 1995.

[28] Kraus, J.D. Antennas for All Applications. 3rd ed. The USA, McGraw-Hill. 2002. 921 p.

[29] Rao KS, Nikitin PV, Lam SF. Antenna design for UHF RFID tags: A review and a practical application. IEEE Transactions on antennas and propagation. 2005 Dec;53(12):3870-6.

[30] Seiko Instruments. Datasheet: Cheap Type Electric Double Layer Capacitor CPH3225A/CP3225A; 2010 [cited 2011]; Available from: http://www.sii-me.com

[31] Agago Technologies. Datasheet: HSMS-286x Series Surface Mount Microwave Schottky Detector Diodes; 2006 Aug 22. Available from: https://www.broadcom.com/products/wireless/diodes/schottky/hsms-2862

[32] Agilent Technologies. Datasheet: Diode Detector Simulation using Agilent Technologies EEsof ADS Software; 1999. Available from: http://www.g3ynh.info/circuits/diode_data/AN1156.pdf

[33] Skyworks. Datasheet: SMP1340 Series: Fast Switching Speed, Low Capacitance, Plastic Packaged PIN Diodes; 2017 May 24. Available from: http://www.skyworksinc.com/uploads/documents/200051J.pdf

[34] Björninen T, Virkki J, Sydänheimo L, Ukkonen L. Impact of recurrent stretching on the performance of electro-textile UHF RFID tags. InElectronics System-Integration Technology Conference (ESTC), 2014 Sep 16 (pp. 1-5). IEEE.